

77
ARL-TDR-62-24

~~163~~ 13209

CODE
2A

MEASUREMENT OF SOLAR FLARE PRODUCED
COSMIC RADIATION

dePaul J. Corkhill, Major, USAF, VC
Rudolf A. Hoffman, Captain, USAF, VC
Robert J. Lockhart, S/Sgt, USAF

TECHNICAL DOCUMENTARY REPORT NO. ARL-TDR-62-24

October 1962

6571st Aeromedical Research Laboratory
Aerospace Medical Division
Air Force Systems Command
Holloman Air Force Base, New Mexico

Project 6892, Task 689206

FACILITY FORM 802

| | |
|-------------------------------|------------|
| N 65 16477 | |
| (ACCESSION NUMBER) | (THRU) |
| 177 | 1 |
| (PAGES) | (CODE) |
| CP 50114 | 29 |
| (NASA CR OR TMX OR AD NUMBER) | (CATEGORY) |

GPO PRICE \$ _____

OTS PRICE(S) \$ _____

Hard copy (HC) 3.00

Microfiche (MF) 75

~~SECRET~~

Qualified requesters may obtain copies of this report from ASTIA. Orders will be expedited if placed through the librarian or other person designated to request documents from ASTIA.

This document may be reproduced to satisfy official needs of US Government agencies. No other reproduction authorized except with permission of 6571st Aeromedical Research Laboratory, Holloman AFB, New Mexico.

When US Government drawings, specifications, or other data are used for any purpose other than a definitely related government procurement operation, the government thereby incurs no responsibility nor any obligation whatsoever; and the fact that the government may have formulated, furnished, or in any way supplied the said drawings, specifications, or other data is not to be regarded by implication or otherwise, as in any manner licensing the holder or other person or corporation, or conveying any rights or permission to manufacture, use, or sell any patented invention that may in any way be related thereto.

This document made available for study upon the understanding that the US Government's proprietary interests in and relating thereto, shall not be impaired. In case of apparent conflict between the government's proprietary interests and those of others, notify the Staff Judge Advocate, Air Force Systems Command, Andrews Air Force Base, Washington 25, D. C.

Do not return this copy. Retain or destroy.

SECRET


FOREWORD

Description of equipment and circuit diagrams for the Lockheed detection systems were obtained from the report "Operating and Maintenance Manual for Radiation Detection Equipment", which was published in fulfillment of Contract AF 29(600)-2361, (1962), Lockheed Missiles and Space Company.

The results and discussion were obtained in part from the report "Radiation Measurements with Balloons, 1961," 2-64-62-1, March 1962, Lockheed Missiles and Space Company, (AF 29(600)-2361).

Information on the balloons and associated equipment was excerpted from the "Final Report" required by Contract AF 29(600)-2994, October 1961, Raven Industries, Inc., Sioux Fall, South Dakota.

This investigation was supported in part by the National Aeronautics and Space Administration (Order R-12).



ABSTRACT

13903
16477

To determine the intensity and energy spectrum of radiation in the atmosphere following a solar flare, an instrument package consisting of a scintillation telescope (for protons), low and high energy neutron detectors and a shielded Geiger Counter was designed and built. The system was carried to altitudes of 120,000 to 130,000 feet by polyethylene balloons on two occasions during July 1961. On a third flight, which took place during conditions of very high radiation in the atmosphere due to a solar flare, the balloon ruptured at 90,000 feet, so data were obtained on this flight for only a short time. A malfunction in the Geiger Counter circuitry and in the power supply of the scintillation telescope rendered almost all these data unreliable. Useful data from the neutron detectors were obtained during the early hours of each flight. The neutron data which were obtained compared well with calculated spectrum curves.

Author

PUBLICATION REVIEW

This technical documentary report has been reviewed and is approved.

[Signature]

HAMILTON H. BLACKSHEAR
Lt Colonel, USAF, MC
Commander,
6571st Aeromedical Research Laboratory

TABLE OF CONTENTS

| | Page |
|---|------|
| I. INTRODUCTION | 1 |
| II. METHODS | 3 |
| A. Radiation Detection System | 3 |
| 1. Scintillation Telescope | 3 |
| 2. Neutron Detectors | 7 |
| B. Data Acquisition System | 7 |
| C. Balloon Flights | 10 |
| III. RESULTS AND DISCUSSION | 12 |
| IV. CONCLUSIONS | 34 |
| V. FUTURE PLANS | 34 |
| VI. RECOMMENDATIONS | 35 |
| REFERENCES | 37 |
| APPENDIX | |
| A. RADIATION DETECTION SYSTEM CIRCUITRY | 39 |
| B. DETAILED DISCUSSION OF DATA ACQUISITION EQUIPMENT AND PROCEDURES | 47 |
| C. BALLOON CONSTRUCTION AND PAYLOAD WEIGHTS | 69 |

LIST OF ILLUSTRATIONS

| Table | Page |
|---|------|
| I. Solar Flares Observed During July 1961 by Sacramento Peak Observatory | 2 |
| II. Transmitter Characteristics with Various Operating Voltages | 59 |
| III. Ground Receiving Station Equipment | 60 |
| IV. Monitoring and Test Equipment | 61 |
| V. Airborne Receiving Station Equipment | 65 |

Figure

| | |
|---|----|
| 1. Proton Telescope Detector | 4 |
| 2. Energy Loss in Thin Crystal Versus Energy Loss in Thick Crystal | 5 |
| 3. Block Diagram of Counter-Telescope Electronics. . | 6 |
| 4. Front View of Lockheed Detector Package | 8 |
| 5. Rear View of Lockheed Detector Package | 9 |
| 6. Block Diagram of the Data Reduction System. . . . | 13 |
| 7. Time and Altitude History of Counting Rate in Neutron Detector A for Flight 1 | 17 |
| 8. Time and Altitude History of Counting Rate in Neutron Detector B for Flight 1 | 18 |
| 9. Comparison of Counting Rates Observed in Neutron Detectors A and B for Flight 1 | 19 |
| 10. Time and Altitude History of Counting Rate in Neutron Detector A for Flight 2 | 20 |
| 11. Time and Altitude History of Counting Rate in Neutron Detector B for Flight 2 | 21 |

| Figure | Page |
|---|------|
| 12. Comparison of Counting Rates Observed in Neutron Detectors A and B for Flight 2 | 22 |
| 13. Time and Altitude History of Counting Rate in Neutron Detector A for Flight 3 | 23 |
| 14. Time and Altitude History of Counting Rate in Neutron Detector B for Flight 3 | 24 |
| 15. Comparison of Counting Rates Observed in Neutron Detector A and B for Flight 3 | 25 |
| 16. Spectrum Observed in Proton Telescope in the Altitude Interval 10,000 to 98,000 Feet for Flight 3 | 27 |
| 17. Spectrum Observed in Proton Telescope at Ceiling for Flight 3 | 28 |
| 18. Time and Altitude History of Counting Rate in Proton Telescope for Flight 3 | 29 |
| 19. Temperatures Observed During Flight 3 | 30 |
| 20. Temperatures Observed During Flight 1 | 31 |
| 21. Temperatures Observed During Flight 2 | 32 |
| 22. Section of Oscillographic Record from Flight 1 | 33 |
| 23. Block Diagram of Neutron Detector Electronics | 40 |
| 24. Photomultiplier Detector for Proton Telescope | 41 |
| 25. Neutron Phoswich | 42 |
| 26. Boxcar Rundown Generator | 43 |
| 27. Phoswich Count Rate Meter | 44 |
| 28. Telescope Logic Circuit Board 3 | 45 |
| 29. Count Rate Meters Board 4 | 46 |
| 30. Top View of Telemetry Transmission System | 48 |

| Figure | Page |
|---|------|
| 31. Top View of Battery Box | 49 |
| 32. Signal Input Strip on End of Battery Box | 50 |
| 33. Telemetry Transmission Antenna | 51 |
| 34. Telemetry Van | 53 |
| 35. Block Diagram of Ground Receiving Station | 54 |
| 36. Layout of Telemetry Van | 55 |
| 37. Tape Recorder | 56 |
| 38. Cabinet 1, Telemetry Ground Station | 57 |
| 39. Cabinet 2, Telemetry Ground Station | 58 |
| 40. Air Force Tracking Aircraft | 62 |
| 41. Block Diagram of Airborne Receiving Station | 63 |
| 42. The Airborne Receiving Station | 64 |
| 43. Balloon Payload Ready to Launch | 67 |
| 44. Signal Strength Recordings | 68 |

MEASUREMENT OF SOLAR FLARE PRODUCED COSMIC RADIATION

I. INTRODUCTION

The future space traveler may anticipate encountering radiation from four main sources: (1) galactic cosmic rays, (2) radiation from the quiescent sun, (3) solar flare radiation, and (4) the Van Allen Belts. Biological effects of the first two are presently thought to be insignificant, while the dangers of the last may be minimized by shielding and appropriate choice of trajectory. This leaves the solar flare as perhaps the most important originator of biologically damaging particles (Ref. 1).

Solar flares appear to occur most often on surface areas of the sun containing the larger sunspot complexes (Ref. 2). It is believed that sunspots are the result of a flow of solar gases into a low pressure area. The resultant cooling of the gases by expansion appears as a dark spot on a photograph of the sun's disc. Although normally lasting only a few days, the largest groups of sunspots may persist long enough to appear two or more times as the sun passes through an average rotational period of 27 days. The variation of the number of sunspots with time reaches a maximum approximately every 11 years, while the maxima appear to vary gradually with a period in excess of 100 years. The current 11-year cycle reached the highest maximum in the last 200 years during March 1958. It is anticipated that the maxima will decrease for the next 50 years or more, reaching a value in the long term variation less than one quarter of the March 1958 peak.

A flare appears as an increase in brightness of the area around a sunspot group, which reaches a peak in a few minutes, then gradually decays. The smallest flares (Class 1) have a mean life of 15 minutes and are very numerous, while the largest (Class 3+) last about 3 hours, but occur on an average of only once or twice a year. Ten percent of the flares of Classes 3 and 3+ produce within a few hours of occurrence a substantial increase in cosmic ray activity in the earth's atmosphere. These rays appear to be predominantly protons with energies up to 20 billion electron volts from the highest energy flares. The positively charged particles are deflected toward the polar regions by the earth's magnetic field. Thus, for balloon experimentation, activity increases with altitude and at higher geomagnetic latitudes (Ref. 3).

The prediction of solar flare activity is based largely on three empirical facts: (1) a solar disc free of sunspots will not produce a flare, (2) a sunspot region which has produced flares will likely produce more. A region which has disappeared as a result of solar rotation, will reappear at a predictable time and may then produce more flares, and (3) the current position on the 11-year cycle will determine the relative frequency of occurrence. During the last minimum (1952-1955), only one flare occurred which produced cosmic ray activity. Twenty-five such flares occurred during the last maximum (1957-1958). The experiments described in this report were carried on at a time when sunspot activity was more than half-way down from the March 1958 peak toward the next minimum, which will occur about June 1964. The solar flare activity during July 1961, as presented in Table I was surprisingly high and presented the opportunity to obtain some valuable radiation data.

TABLE I
SOLAR FLARES OBSERVED DURING JULY 1961
BY SACRAMENTO PEAK OBSERVATORY

| <u>Date</u> | <u>Class of Flare</u> | <u>(Duration - UT)</u> |
|-------------|-----------------------|------------------------|
| 11 July | 3 | 1654 - 1916 |
| 12 July | 1 | 2248 - 2315 |
| 15 July | 3+ | 1434 - 1857 |
| | 2 | 1508 - 1542 |
| | 1 | 1613 - 1644 |
| 16 July | 2 | before 1950 - 2106 |
| 17 July | 1 | |
| | 1 | |
| | 1 | |
| 20 July | 2 | 1600 - after 1603 |
| | 2 | before 1832 - 1859 |
| 21 July | 2 | 1714 - 1734 |
| 24 July | 3 | 1722 - after 2214 |
| 28 July | 3 | 1512 - 1938 |

Upon entering the earth's atmosphere, primary cosmic particles transfer their energy by ionization or by collision with the nuclei of oxygen and nitrogen atoms. Above 140,000 feet cosmic radiation intensity in the atmosphere nearly equals the primary flux in free space. By the time the rays have penetrated to 75,000 feet, they have been almost completely converted to secondary radiation (largely neutrons). The total particle flux is inversely proportional to altitude from 140,000 to about 65,000 feet where it reaches a maximum and then drops off to a sea level value of about 2 percent of the maximum.

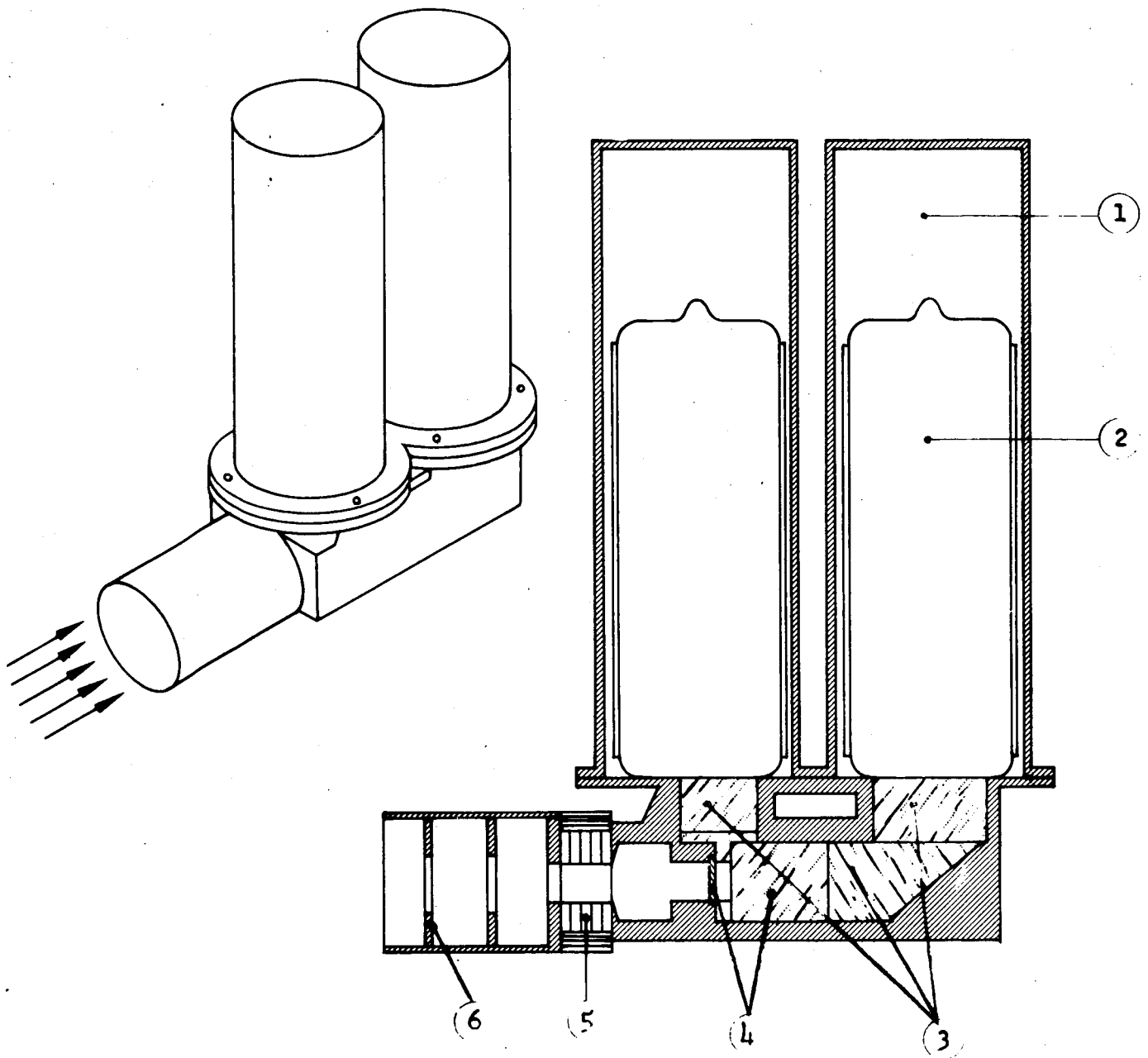
II. METHODS

A. Radiation Detection System

1. The Scintillation Telescope

The primary instrument in the system is a dE/dx and E^* scintillation telescope which was designed to measure the spectrum of protons in the energy range 10 to 200 Mev. The sensing elements of the telescope consist of a thin (0.84 g/cm^2) CsI crystal followed by a thick (13 g/cm^2) CsI crystal. The light output of each crystal is optically piped to the respective photomultiplier. Figure 1 illustrates the size, shape and relative position of the crystals which geometrically define a solid angle of acceptance. The brass collimator serves as a shield to reduce the single rate produced by particles entering the detector crystals from lateral directions. Depending upon their energy and species, incident particles will (1) be stopped in the thin crystal, (2) be stopped in the thick crystal, or (3) traverse both crystals. A plot of the energy loss in the thin crystal versus energy loss in the thick crystal (Figure 2) indicates that the solution of both the energy and the species of the particle can be achieved in certain ranges of the atomic number Z and energy E . The functional block diagram of Figure 3 shows the processing of the responses from the two crystals for subsequent presentation to telemetry. The pulses from each photomultiplier are amplified and stretched on a time base by the "boxcar" generators, whose outputs are gated by the coincidence circuit. Upon superposition in the adding circuit the information from the two crystal sensors is conveyed to one output channel. Despite the superposition, the identity of the separate inputs is retained for subsequent analysis.

* dE/dx crystal - measures rate of energy loss of incident radiation
"E" crystal - total energy of particle minus that lost in dE/dx crystal.



1. Electronics
2. Photomultipliers
3. Light Pipes
4. CsI (Tl) Scintillator
5. Magnet
6. Collimator and Baffles

Figure 1. Proton Telescope Detector

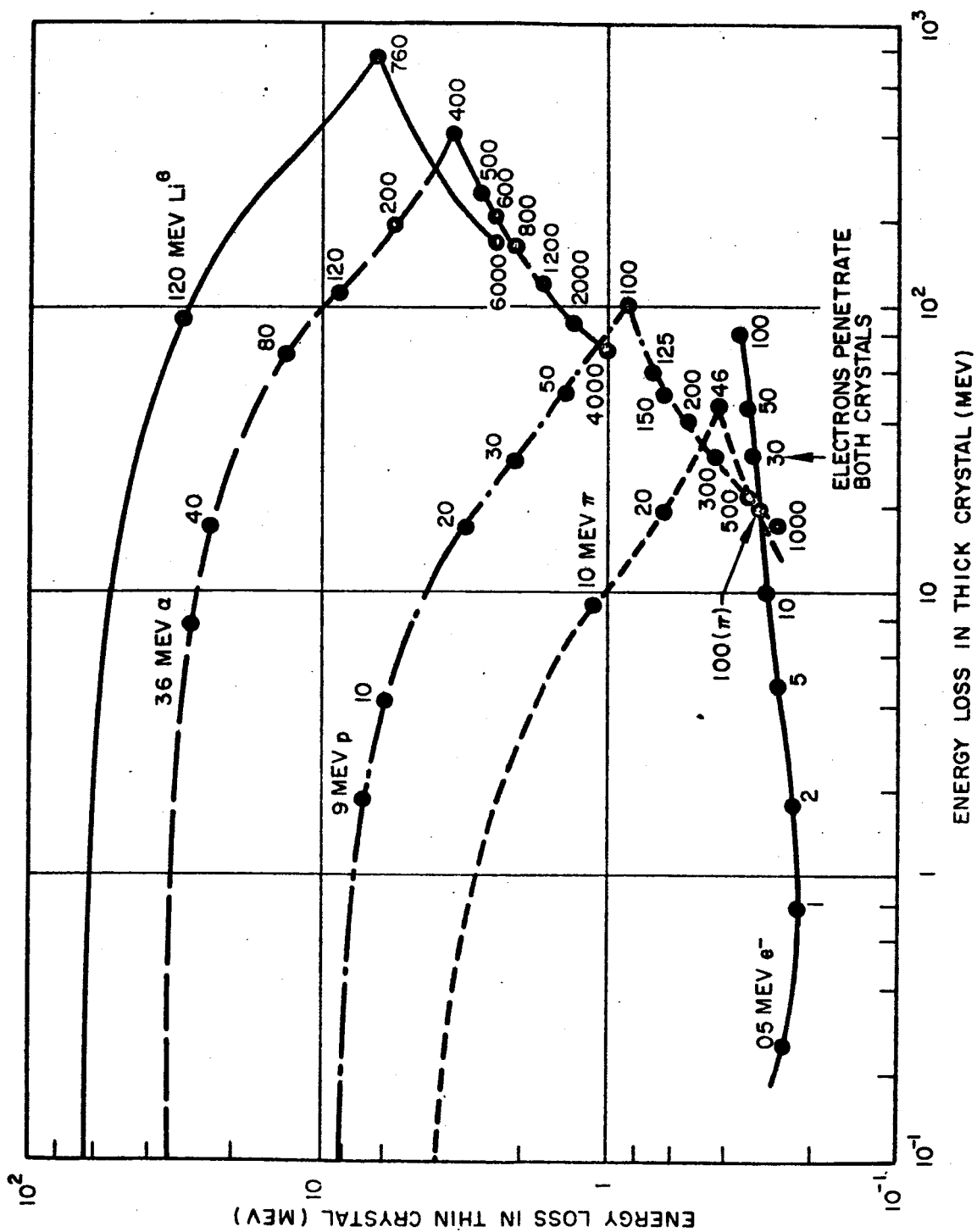


Figure 2. Energy Loss in Thin Crystal Versus Energy Loss in Thick Crystal

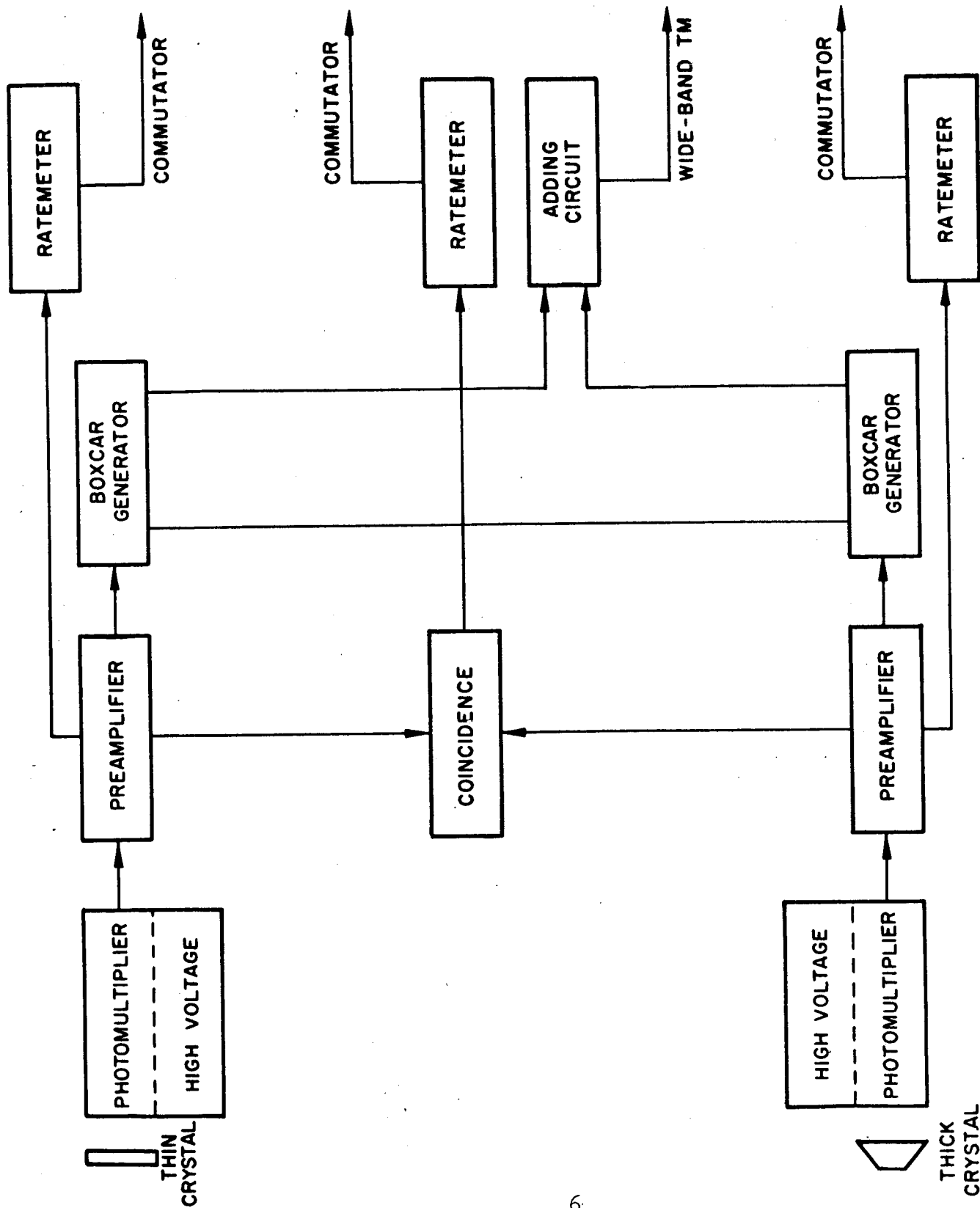


Figure 3. Block Diagram of Counter-Telescope Electronics

2. Neutron Detectors

In order to provide some measure of the neutron spectra encountered, two detectors were used. They were identical except for the shielding surrounding the crystals. The low energy detector had only a light aluminum can around the plastic LiI crystal, while the high energy detector made use of a large polyethylene moderator to extend its counting efficiency to higher neutron energies.

The basic signal of the neutron detector arises from a Li^6I crystal surrounded by a plastic scintillator. Neutrons will induce alpha particles in Li^6 by an (n, alpha) reaction with a Q value of 4.8 Mev. The efficiency of this process is about one percent for neutrons below 1 Mev. The neutron flux is determined by counting the alpha particles. The plastic scintillator serves to distinguish neutrons from energetic charged particles (e.g. protons) which will produce pulses in both scintillators. Because of the difference in fluorescent characteristics of LiI and the plastic scintillators, it is possible for one photomultiplier tube to "look" at both scintillators. The fast plastic pulse is distinguishable from the relatively slow pulse in the LiI crystal. Slow pulses from the LiI are counted in anticoincidence with fast pulses from the plastic. Incident gamma rays or capture gammas in the plastic scintillator will be detected in the LiI crystal through photoelectric capture, Compton scattering or pair production, but these pulses can be rejected through pulse height discrimination. The LiI crystal must be small enough so that an electron cannot lose 4 Mev in traversing it, since such an event might be confused with the alpha pulse induced by a neutron.

Front and rear views of the complete detection system are shown in Figures 4 and 5. The box at the bottom contains the battery pack.

B. Data Acquisition System

The information accumulated by the detection system described above, as well as from other small detectors provided by interested military and civilian organizations, was presented to the telemetry transmission system in the form of DC voltages covering the range 0 to 5 volts. These voltages were converted to proportional frequencies and used to frequency modulate a carrier of 249.9 mc, which was broadcast by a 2-watt transmitter. The transmission system was powered by a pack of 17 silver-zinc wet cells. The antenna was an omnidirectional disccone type with unity gain.

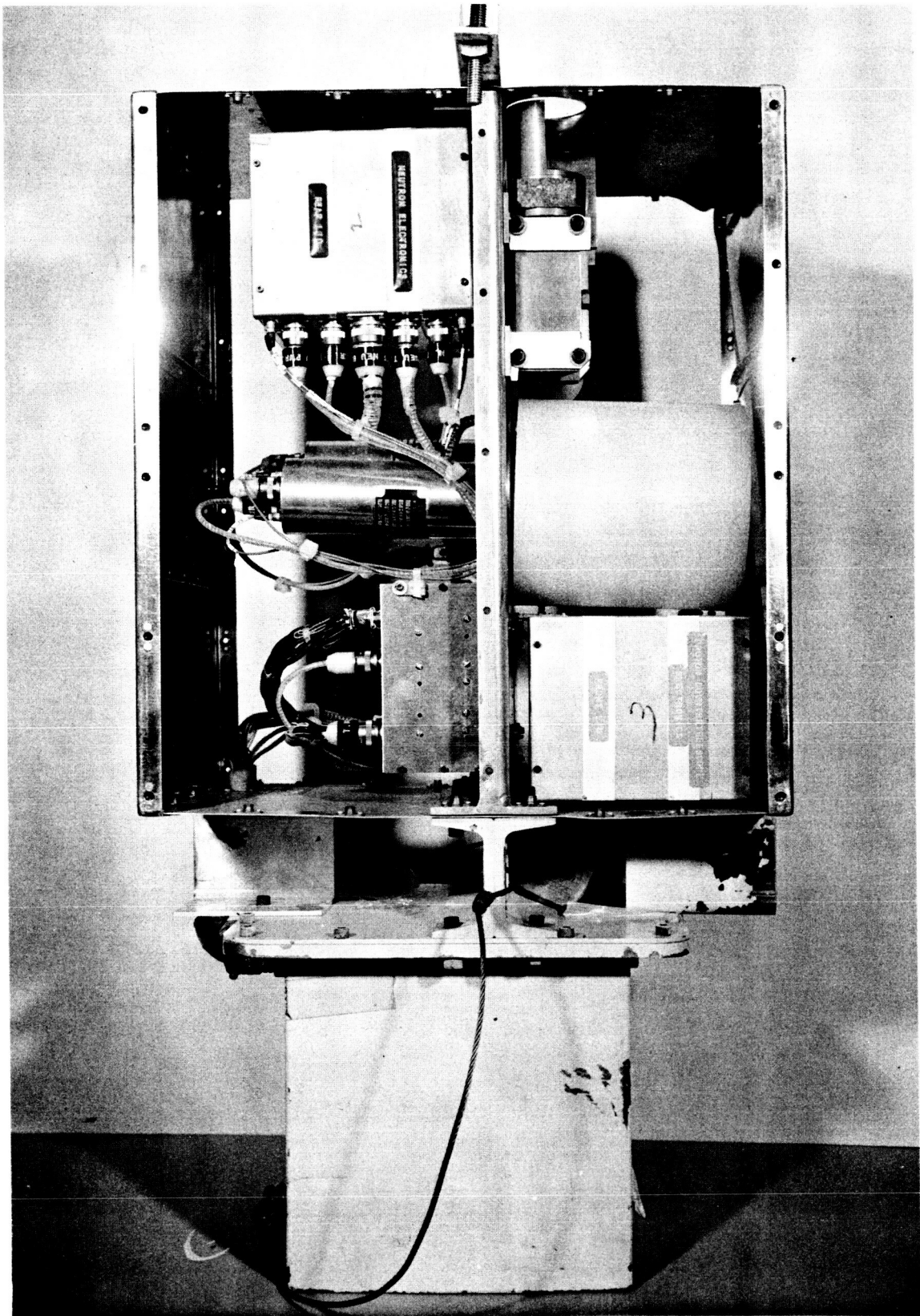


Figure 4. Front View of Lockheed Detector Package

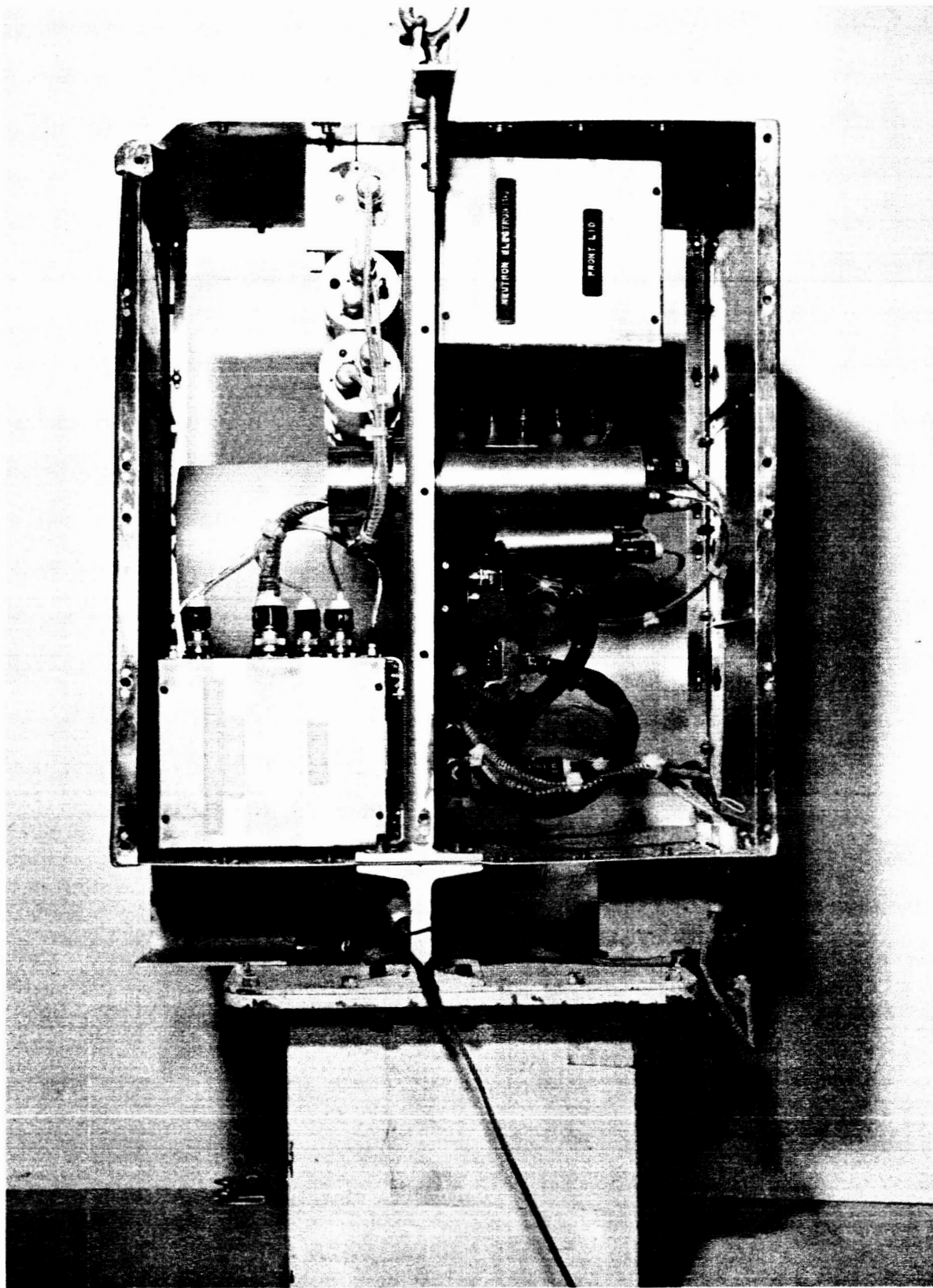


Figure 5. Rear View of Lockheed Detector Package

The primary telemetry receiving station was housed in a small van at the launch site, Bemidji, Minnesota airport. The incoming signal was picked up by a helical antenna on the van roof, then cabled to a preamplifier and telemetry receiver. The composite signal was recorded directly on a 14-track tape recorder operating at 7-1/2 inches/second (frequency response 300 to 31,000 cps). In addition, five channels of data were discriminated and recorded on individual tracks. Balloon altitude in the form of Morse code, WWV time* and voice commentary were also recorded. The strength of the telemetry signal was recorded directly from the receiver by a strip chart recorder. This signal indication was used to reposition the receiving antenna at frequent intervals. Monitoring of the data from the tape reproduction facilities was accomplished by an oscillographic recorder.

A secondary receiving station of somewhat lesser complexity was installed in the Air Force tracking aircraft. It consisted of a small stub antenna, receiver and 7-track tape recorder. To permit an economical tape speed (15 inches/second), two of the high-frequency data channels were discriminated and recorded separate from the composite signal. WWV time and voice commentary were also recorded. The only data monitoring facility was a dual-channel oscilloscope.

C. Balloon Flights

Manufacture of the balloons, and launch, tracking and recovery of the payload were carried out by Raven Industries, Sioux Falls, South Dakota, under Contract AF 29(600)-2994. The balloons were manufactured from 3/4-mil polyethylene film, with volumes of 13.5 million cubic feet for the first flight and 6 million cubic feet for the other flights.

Numerous types of equipment designed to control the actions of the balloons were provided by the contractor. Two types of automatic ballast controls were used to maintain a constant rate of ascent and a relatively constant float altitude. A drive-up ballast was automatically released by a timer upon reaching a preset altitude. A dribble ballast periodically released a slow flow of steel grit at a rate of approximately five pounds per minute to keep the balloon stabilized. To prevent the balloons from becoming a hazard to aircraft, two switches were incorporated, one to cut down the payload if the balloon failed to reach 44,000 feet within two hours, the other to effect cutdown if the flight train drifted down to 44,000 feet.

* National Bureau of Standards time service

Three devices were provided for terminating a normally operating flight. Two of these, one motor driven and one driven by a clock mechanism, operate on the principle of a stylus moving in a helical groove while a moving arm contacts a fixed one to complete an electrical circuit. The third device was a transistorized radio command receiver which could override the two timer circuits and cut loose the payload at any desired time. The receiver responded only to a coded signal in order to prevent unauthorized operation. Upon activation of any of the termination devices, a battery fired an explosive charge which severed the main load line, allowing the equipment to descend by parachute.

A Bendix-Friez bellows, accurate from ground level to 100,000 feet, and a Kollsman SK-901, accurate from 70,000 feet upward were used to obtain altitude data. The information was obtained from a code drum and transmitted in the form of Morse code on a frequency of 1.666 mc. Also included in the flight package was a Wallace and Tiernan aneroid gauge which was photographed at various intervals.

Since it is difficult to predict solar flares with any accuracy, the contractor maintained a skeleton crew at Bemidji to initiate the launch procedures immediately after being informed that radiation in the atmosphere was increasing as a result of a solar flare. Other members flew in from Sioux Falls as soon as possible, so that a balloon could be launched within five hours of the occurrence of a flare if this was desirable. Because of the relative scarcity of desirable radiation conditions, launches were made in weather which would normally have forced postponement of a flight. For Flight 1, 18 July 1961, the surface wind was rather high and evidence of a cold front was visible on the horizon. Launch occurred about 7:15 P.M. Central Daylight Time (CDT) and at 9:03 the balloon had reached a peak of 90,000 feet and began to descend. The payload was cut loose and landed in the forest 35 miles from the launch site at 9:50. The reason for the failure was not determined exactly. Radiation in the atmosphere was very high, and the data obtained were very good for the short period involved.

For Flight 2, 20 July 1961, the weather was excellent, and there were no difficulties with the smaller balloon. Launch time was 6:47 P.M. (CDT) and by 9:00 P.M., the balloon had reached 130,000 feet. The telemetry signal was received until 5:00 A.M., 21 July 1961, but the balloon continued to drift until cut down at 1:29 P.M. by the mechanical timer since radio command system failed to function. The payload dropped in the mountains near Kalispell, Montana, from where it was carried out by the recovery crew. The equipment was returned to Bemidji during the evening of 25 July.

The third flight, 28 July 1961, was for control purposes, so atmospheric radiation was nearly normal. There was a light cross wind and low clouds for the early morning launch (5:45). Average altitude was about 124,000 feet. The flight was terminated at 4:00 P.M., although the telemetry signal was still strong.

Detailed information on the construction of the balloons and the weight of items comprising the payloads may be found in Appendix C.

III. RESULTS AND DISCUSSION

The data from detection equipment provided by the University of Minnesota, Hughes Aircraft Company and the Air Force Special Weapons Center were copied from the original tapes onto 1/2-inch magnetic tapes and sent to the sponsoring organizations. These results will not be considered in this report. The data from the Lockheed detection system were also copied onto 1/2-inch magnetic tapes and sent to the Lockheed Missiles and Space Company for reduction. The latter information is presented graphically and discussed in the following sections.

A block diagram of the system used to reduce the data is shown in Figure 6. The neutron data were obtained from the tapes in one of two ways. The first, which is not indicated on the block diagram, was to pass the pulses from the appropriate track through an amplifier and into a 400-channel pulse height analyzer which had been modified to accept the rather long "boxcar" outputs from the neutron detectors. Information was recorded in a particular 100-channel subgroup of the analyzer for a given time (or altitude) interval, at the end of which the pulses were routed into the next 100-channel subgroup. This process was repeated until all four 100-channel subgroups were filled. The tape reproducer was then stopped and the information printed out of the pulse height analyzer.

The second method by which the neutron data were obtained, and which was used only to verify the results already obtained from Flight 1, may best be understood by referring to Figure 6. With the data select switch on one of the neutron channels and the pulse height analyzer gate switch on "off", the long boxcar outputs from the neutron detectors were fed into a microsecond pulse shaping network which sampled the pulse height in the middle of the boxcar pulse as well as shaping it suitably for the following conventional amplifier stage. The information was then recorded on the pulse height analyzer in the same manner as described above:

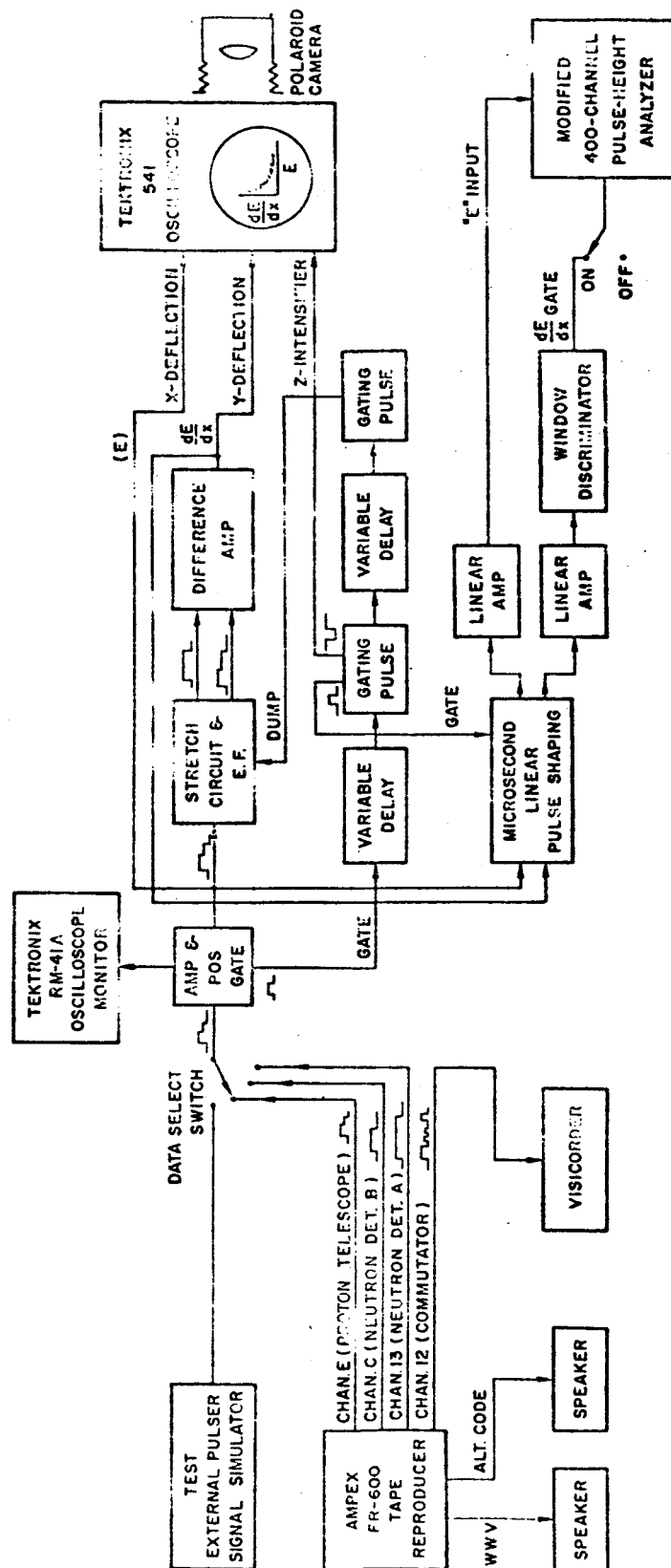


Figure 6. Block Diagram of the Data Reduction System

The second method by which the neutron data were processed was essentially part of the scheme employed to correlate the "dE/dx" and "E" double boxcar pulses obtained from the proton telescope. The first portion of the pulse represents the sum of the pulse heights from the dE/dx and E crystals, and the second portion represents the E pulse height alone. To present the correlated pulse heights, the height of the second portion of the pulse was subtracted from the height of the first portion to obtain the pulse height due to the dE/dx crystal alone. This was accomplished by stretching the summed portion of the proton telescope pulse so that it overlapped the E pulse height portion of the pulse, and then subtracting the unshaped pulse from the stretched pulse, as indicated by the difference amplifier in Figure 6. The latter portion of the wave form appearing at the output of the difference amplifier was then proportional to the dE/dx pulse height. A short sampling pulse was applied during this "latter" time to the wave form appearing at the output of the difference amplifier and to the "original" pulse. This dE/dx and E pulse height information was recorded simultaneously by two methods.

One method of recording the proton telescope data was to display the correlated pulse heights on an oscilloscope. The dE/dx pulses were placed on the vertical deflection plates of the oscilloscope, and the E pulses were placed on the horizontal deflection plates. The Z axis (intensifier) of the oscilloscope was gated by the sampling pulse. Hence, each proton telescope pulse had a unique coordinate on the oscilloscope face, according to its dE/dx and E pulse heights. On the oscilloscope face, each correlated pulse height appeared as a bright dot which could be recorded by a Polaroid camera. If such a photograph were to be analyzed, few enough dots would be recorded so that each dot could be counted individually. The analysis of such a photograph would entail dividing the appropriate area into cells and counting the dots which fell within a given cell. This method has the disadvantage of being tedious, but the advantage of getting all the possible information on one pass through the data (the system is essentially a two dimensional analyzer with a photographic memory). In the present work, this system was used only to survey the data.

The other method of recording the proton telescope data was to store it in the appropriately gated 400-channel analyzer. After the dE/dx and E pulses had been generated, they were fed into two conventional amplifiers, one of which was equipped with a window discriminator. The output of the discriminator was used to gate the analyzer. The E pulses were amplified and

fed into the input of the 400-channel analyzer, and the dE/dx pulses in a particular energy interval (determined by the discriminator settings) gated the analyzer. Thus, the E crystal pulse height spectrum could be obtained in coincidence with any portion of the dE/dx spectrum. The spectra obtained from the telescope on all three flights indicated that most of the information lies along the E axis. All the pertinent data can be obtained for the proton telescope using the second data reduction scheme described. Here all the E pulses which are in coincidence with a dE/dx pulse occurring in the interval bounded by the E axis and the 1.5 cm line are recorded on the analyzer.

The commutated information, which included the outputs from the various count rate meters, as well as the outputs from the thermistors, was recorded approximately every 400 seconds on a Visicorder. The Visicorder recordings were analyzed by hand. The output voltages obtained were converted into counting rates and temperatures with the aid of the known calibrations. The rates indicated by the count rate meters were sufficiently low as to indicate no dead time in the electronics and were not considered further (except for the Geiger Counter). The counting rates observed in the Geiger Counter varied from flight to flight in such a manner as to indicate a malfunction of either the high voltage power supply or the count rate meter associated with the counter. Thus, the Geiger Counter rates were considered unreliable and are not shown.

When the data obtained from all flights were examined in detail, a gain shift was observed in the counters which affected the length of time for which reliable data could be obtained. The decrease in gain corresponded to a decrease in the temperature of the package and was attributed to instability in the high voltage power supplies. Because of the manner in which the equipment was packaged, temperatures below 15°C were not anticipated. However, measurements showed internal temperatures fell below 0°C for substantial parts of two flights. The result was only two to three hours of reliable neutron counting data for these two flights.

The effect of the decreasing gain on the neutron counters was only to limit the time for which data could be obtained, and not to impair the reliability of the data taken during the first hours of the flight. The reason for this was that the pulse height spectrum of each counter was telemetered, so that the integrated counts under the peak, arising from the $\text{Li}^6(n, \alpha)\text{H}^3$ reaction in the detector, could be easily obtained, even though the center position of the peak decreased in voltage as a function of time.

This fact illustrates the advantage of having available a pulse height spectrum from the neutron detectors to help evaluate the data, rather than, for example, having available only a counting rate from a fixed bias count rate meter.

The time and altitude dependence of the counting rates observed in the neutron counters for Flight 1 are shown in Figures 7 and 8. Since the WWV time signal could not be heard during this flight, the time calibration was achieved by noting a noise burst at about the time the launch was expected. This noise burst was then assumed to denote the time of launch at 1918 CDT, and the succeeding times were measured from this point. The double peaking observed in the counting rate of detector A* as a function of time seems to bear out this assumption. The peaks occurred at an altitude of about 60,000 feet, which is the place where the maximum counting rate would be expected. The balloon passed through this altitude on the ascent, and then quickly again on the descent, after having ruptured at about 90,000 feet. A similar double peaking was not observed in the counting rate versus time plot for detector B. The absence of the second peak in this counter is undoubtedly due to the fact that the decrease in gain for the counter had already become appreciable during the time when the second peak would have occurred, and thus the counting rates obtained at these later times are unreliable. The counting rates as a function of altitude for detectors A and B are compared on the semilogarithmic plot in Figure 9. The counting rates observed for Flight 1 are higher than for either Flights 2 or 3, a result expected since Flight 1 occurred during a rather large solar disturbance.

The time and altitude dependence of the counting rates observed in the neutron counters for Flight 2 can be seen in Figures 10 and 11. Again, no data are shown past the point where the gain shifts made the analysis uncertain. The counting rates as a function of altitude for neutron detectors A and B are compared on the semilogarithmic plot in Figure 12.

For flight 3 the counting rates observed in the neutron detectors are shown as a function of time and altitude in Figures 13 and 14. The counting rates as a function of altitude for neutron detectors A and B are compared on the semilogarithmic plot in Figure 15.

*Detector B was a neutron "phoswich" detector, while detector A was an identical unit surrounded by a polyethylene moderator.

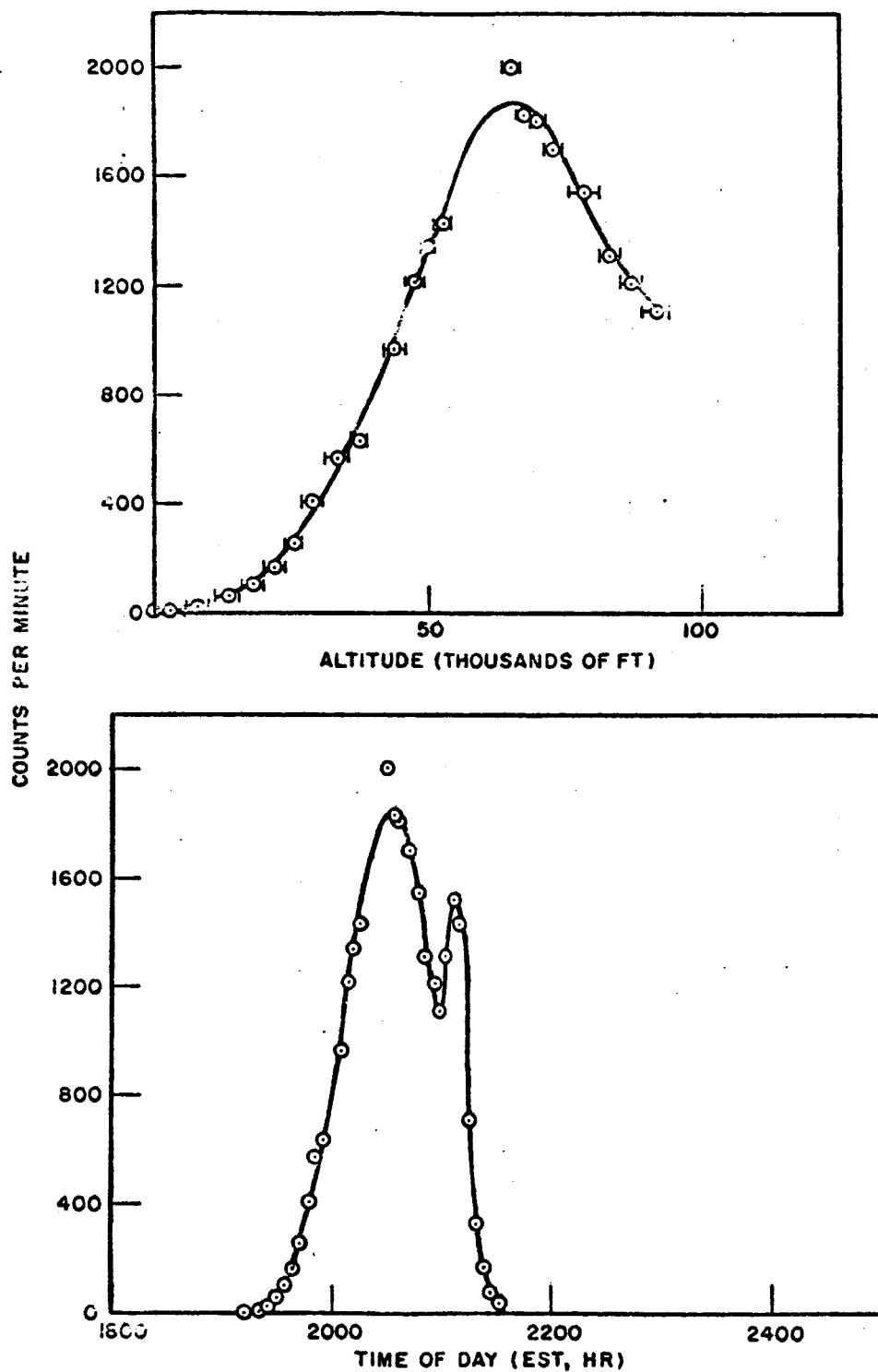


Figure 7. Time and Altitude History of Counting Rate in Neutron Detector A for Flight 1.

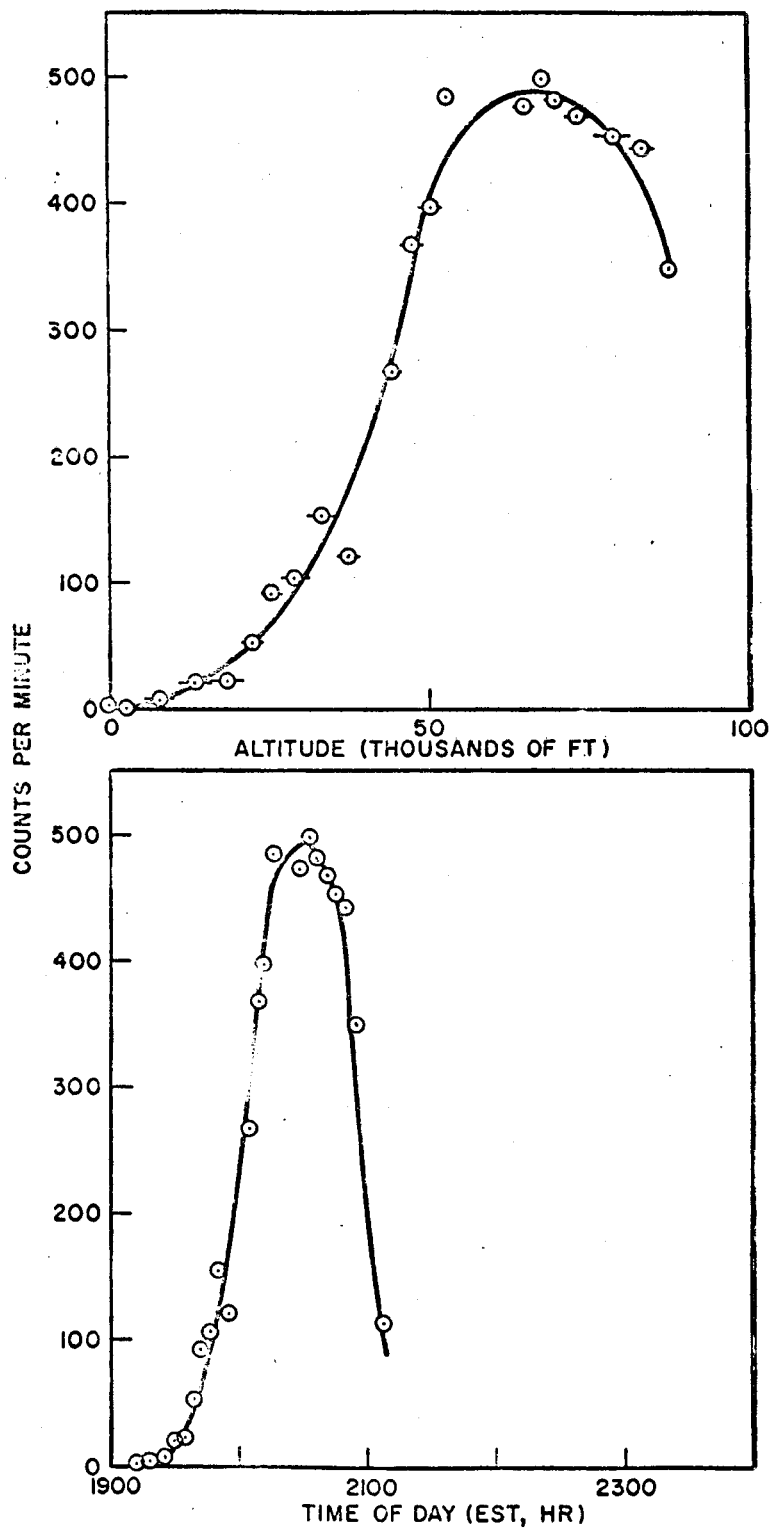


Figure 8. Time and Altitude History of Counting Rate in Neutron Detector B for Flight 1.

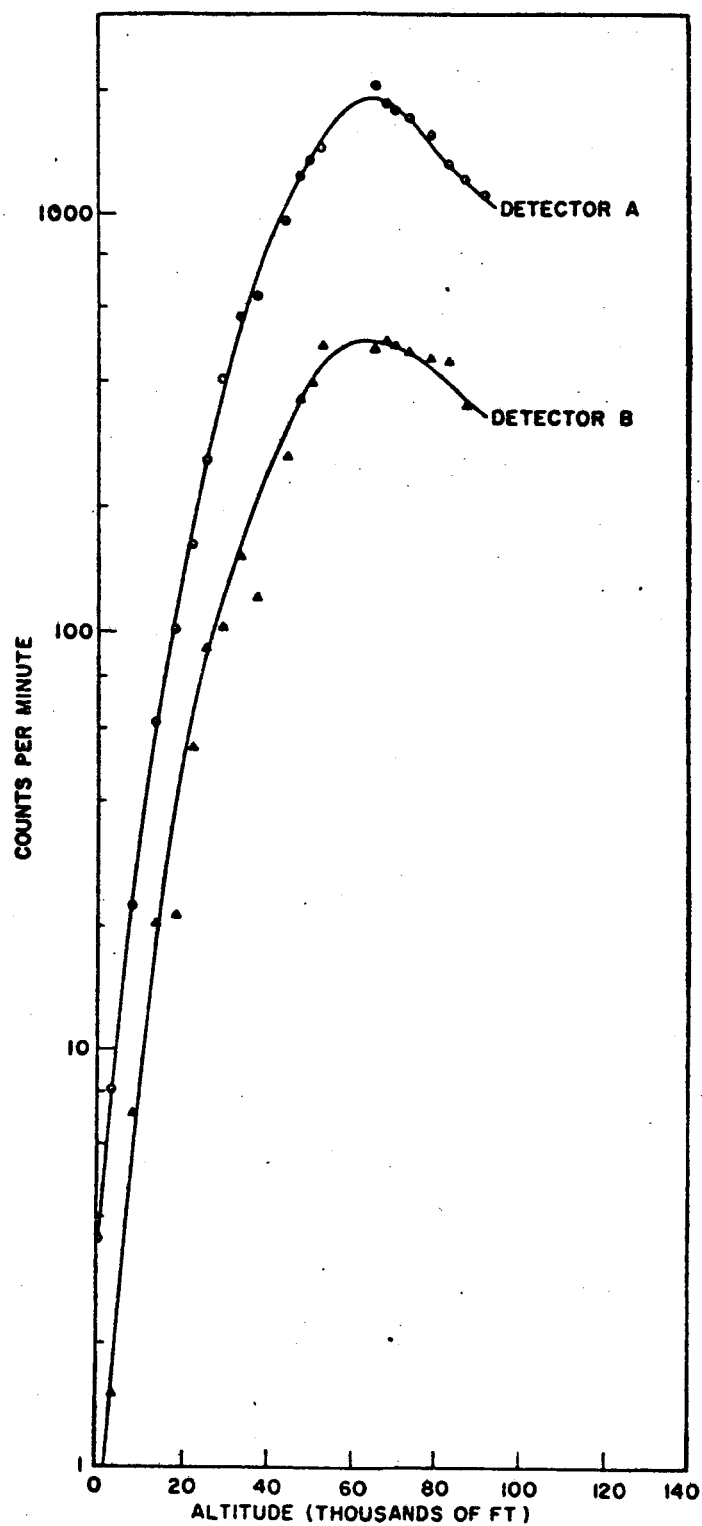


Figure 9. Comparison of Counting Rates Observed in Neutron Detectors A and B for Flight 1.

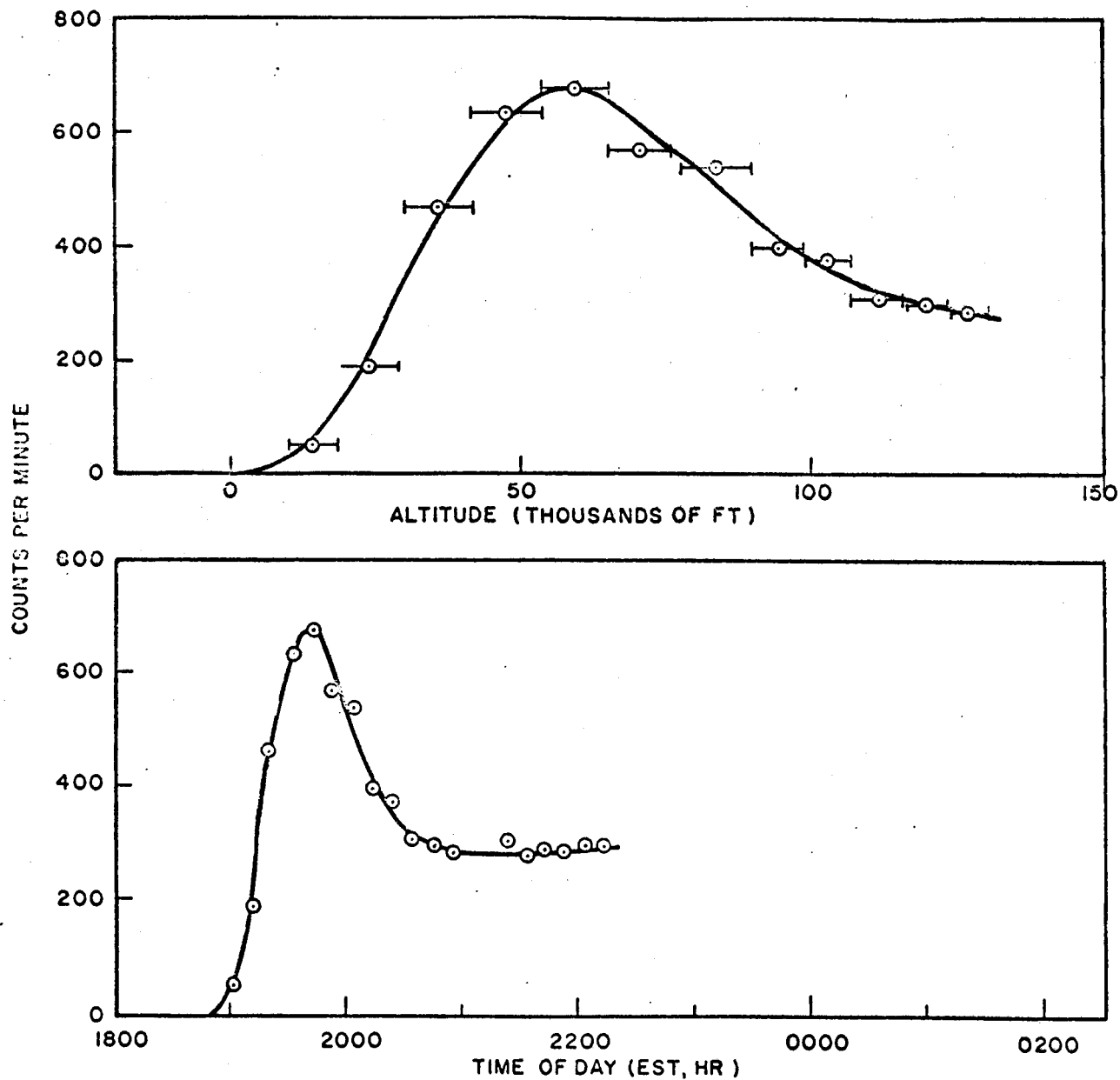


Figure 10. Time and Altitude History of Counting Rate in Neutron Detector A for Flight 2.

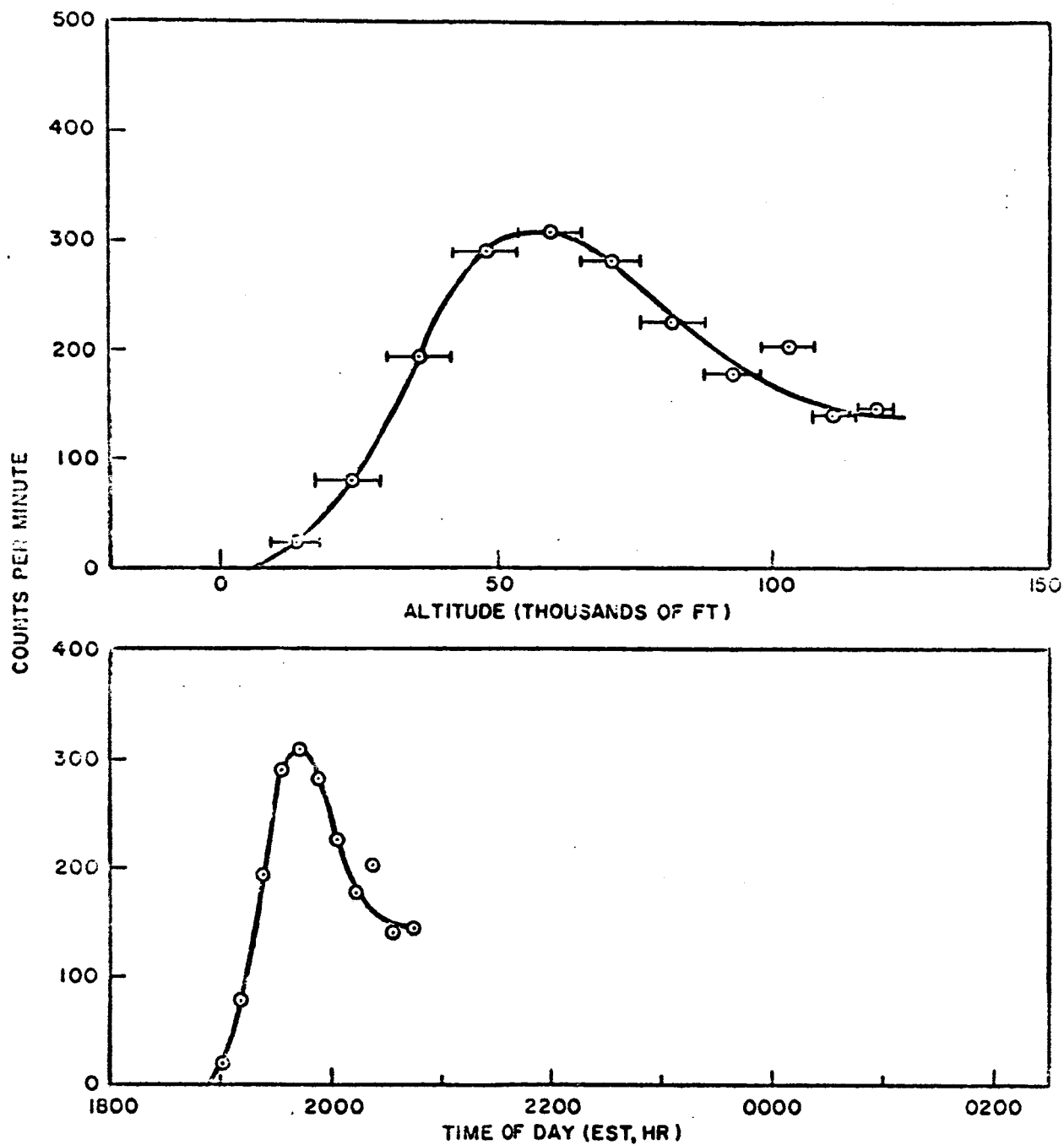


Figure 11. Time and Altitude History of Counting Rate in Neutron Detector B for Flight 2.

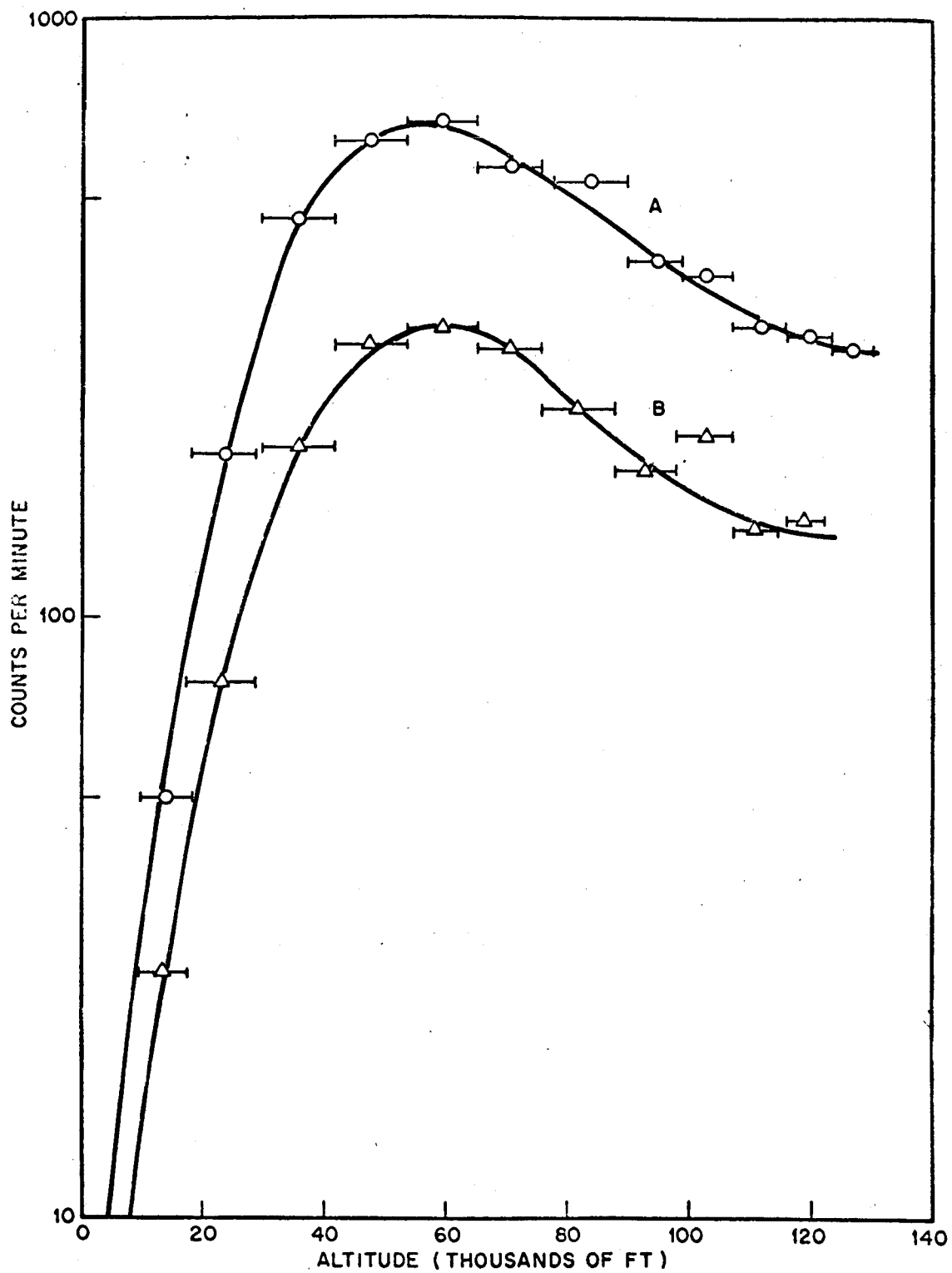


Figure 12. Comparison of Counting Rates Observed in Neutron Detectors A and B for Flight 2.

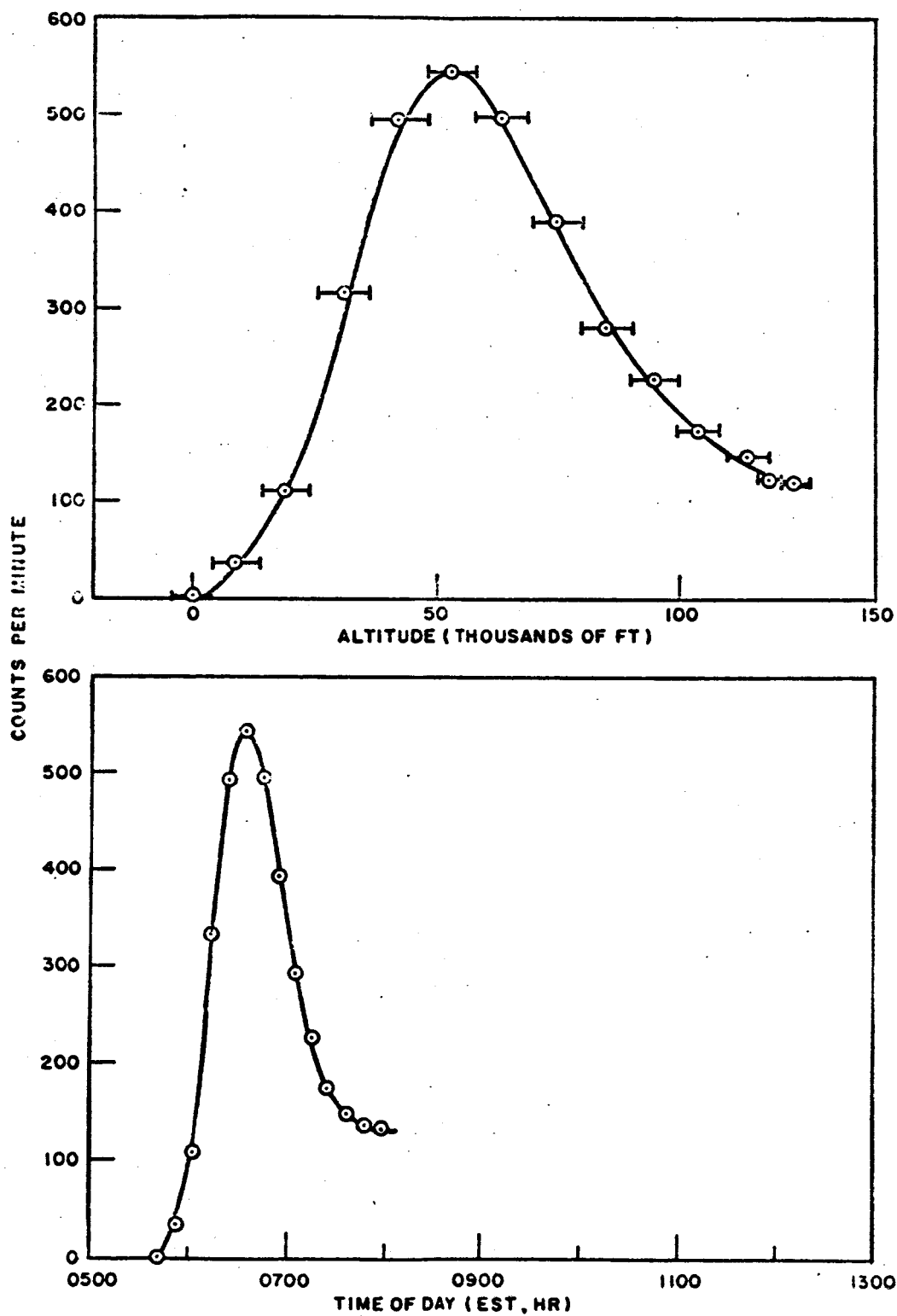


Figure 13. Time and Altitude History of Counting Rate in Neutron Detector A for Flight 3.

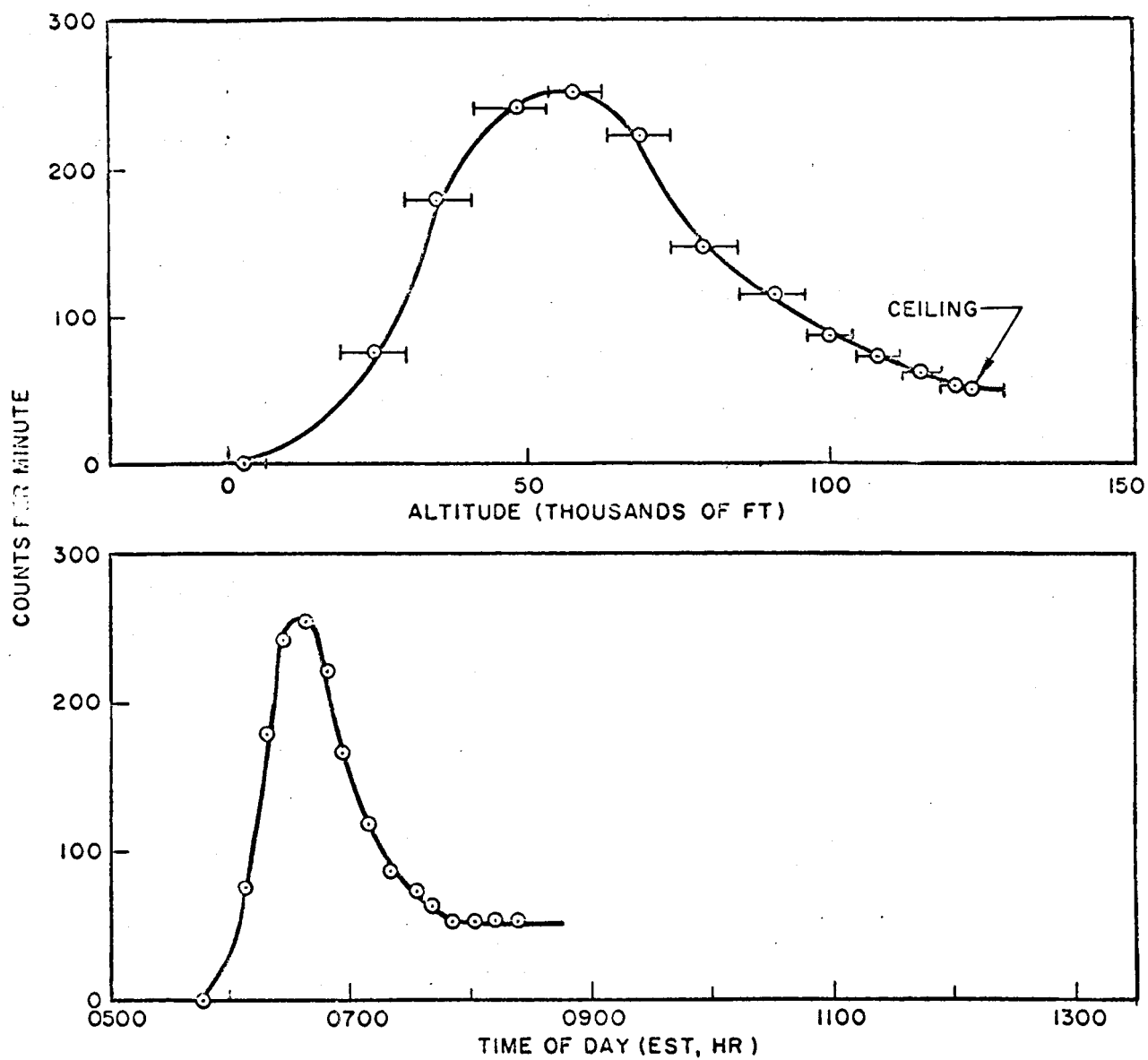


Figure 14. Time and Altitude History of Counting Rate in Neutron Detector B for Flight 3.

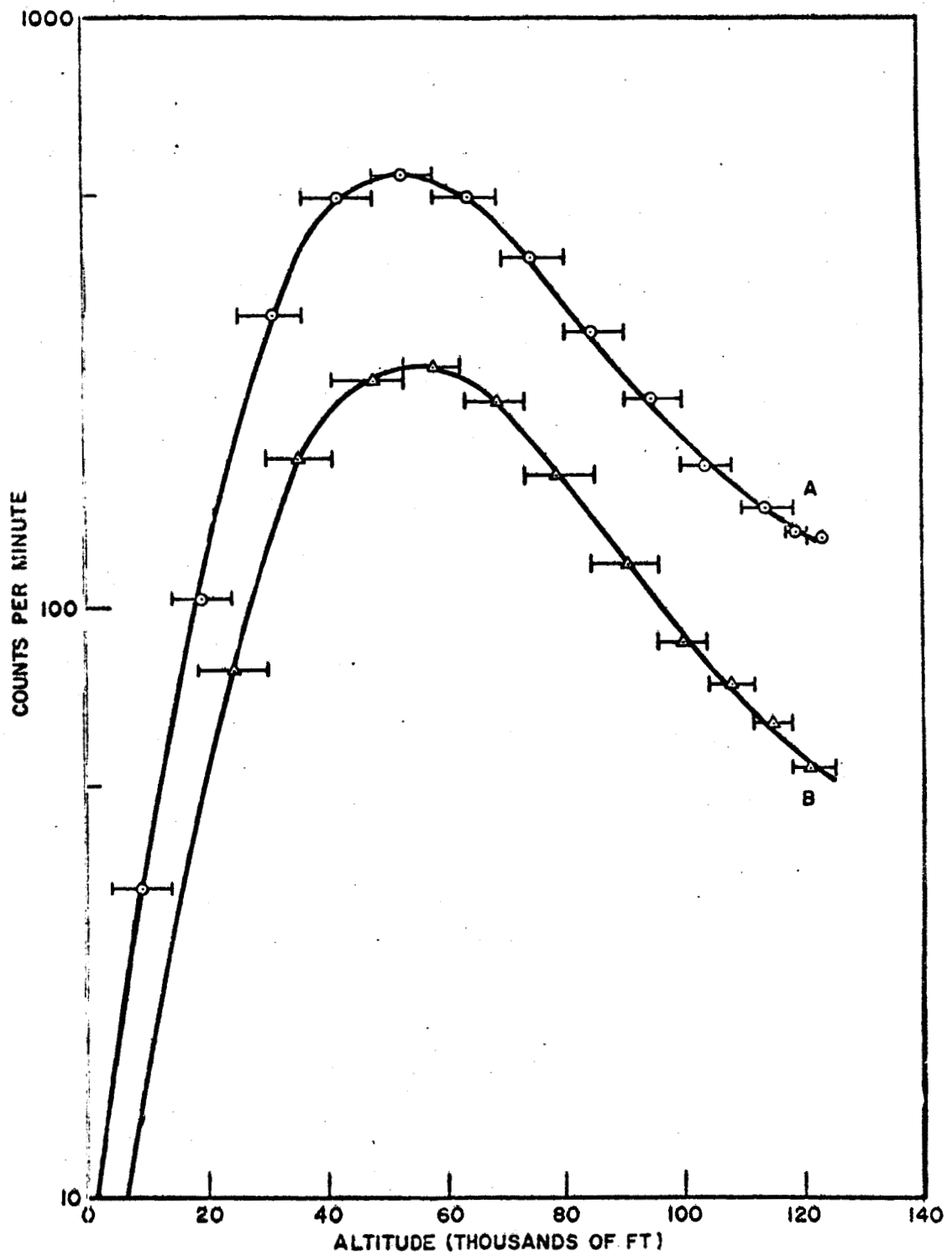


Figure 15. Comparison of Counting Rates Observed in Neutron Detectors A and B for Flight 3.

A summary of the results obtained from the proton telescope is contained in Figures 16, 17, and 18. Figure 16 shows the spectrum in the E crystal which was obtained in the altitude intervals of 10,000 to 98,000 feet; Figure 17 shows the E crystal spectrum which was obtained after the balloon had reached ceiling. These spectra were accumulated on the 400-channel pulse height analyzer, using the coincidence method described above. The spectra observed in the two altitude intervals are similar. Figure 18 shows the integral counting rate after the balloon has reached ceiling. This phenomenon can perhaps best be explained by reference to the temperature variation observed at various places in the package, as shown in Figure 19. In particular, the base (frame) on which the photomultiplier high voltage assembly was attached shows a drastic decrease in temperature (to less than -4°C) at about 0700 CDT and a slow recovery back to the initial temperature at approximately 0930 CDT. The time dependence of the integral counting rate closely parallels the time dependence of the base temperature, the implication then being that the number of proton telescope pulses is a very sensitive function of the temperature. That this indeed should be the case can be seen by recalling that most of the E pulses lay along the E-axis in the "dot representation" of the correlated pulse heights. This fact means that the gain in the dE/dx leg of the circuitry was small enough so that the intrinsic bias present in the telescope electronics was eliminating some of the desired coincidences. Since the dE/dx gain is strongly suspected to decrease with decreasing temperature, the number of E- dE/dx coincidences would vary with temperature in a similar fashion. Thus, the spectra shown (representing an energy interval of 18 to 100 Mev, the energy interval being uncertain to probably a factor of 2) are at best considerably distorted. The base temperature variation for these flights is shown in Figures 20 and 21. It can be seen that the temperature remains below 0°C after the early portion of the flights, a fact which is accounted for since the balloon reached these altitudes during or after sunset. Proton telescope data for Flights 1 and 2 are not presented.

A section of oscillographic record from a magnetic tape of Flight 1 is shown in Figure 22. The numbers refer to the IRIG channels on which the information was telemetered. The complete absence of signal from WWV was characteristic of the entire flight, which took place after a large solar flare.

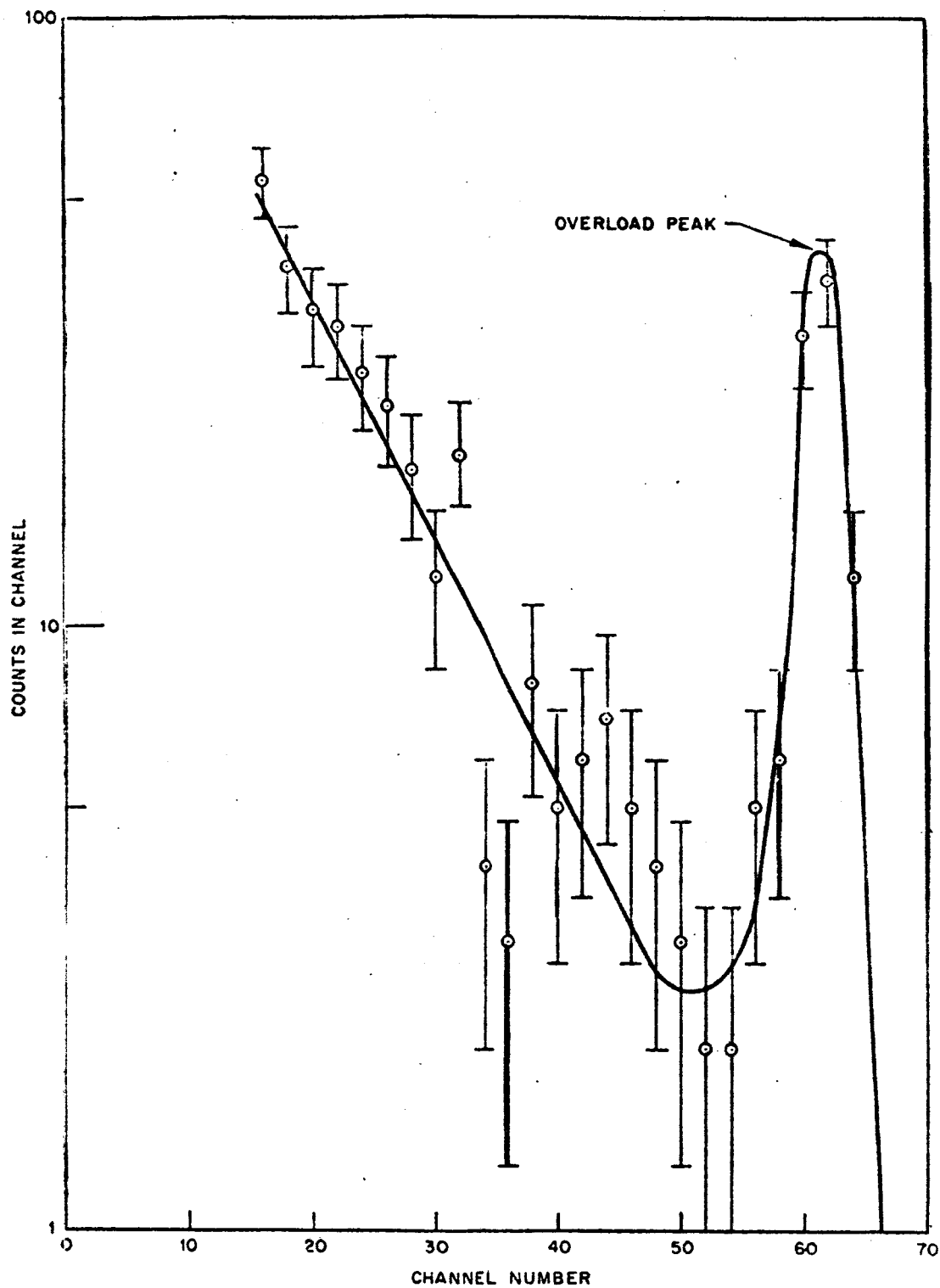


Figure 16. Spectrum Observed in Proton Telescope in the Altitude Interval 10,000 to 98,000 feet for Flight 3.

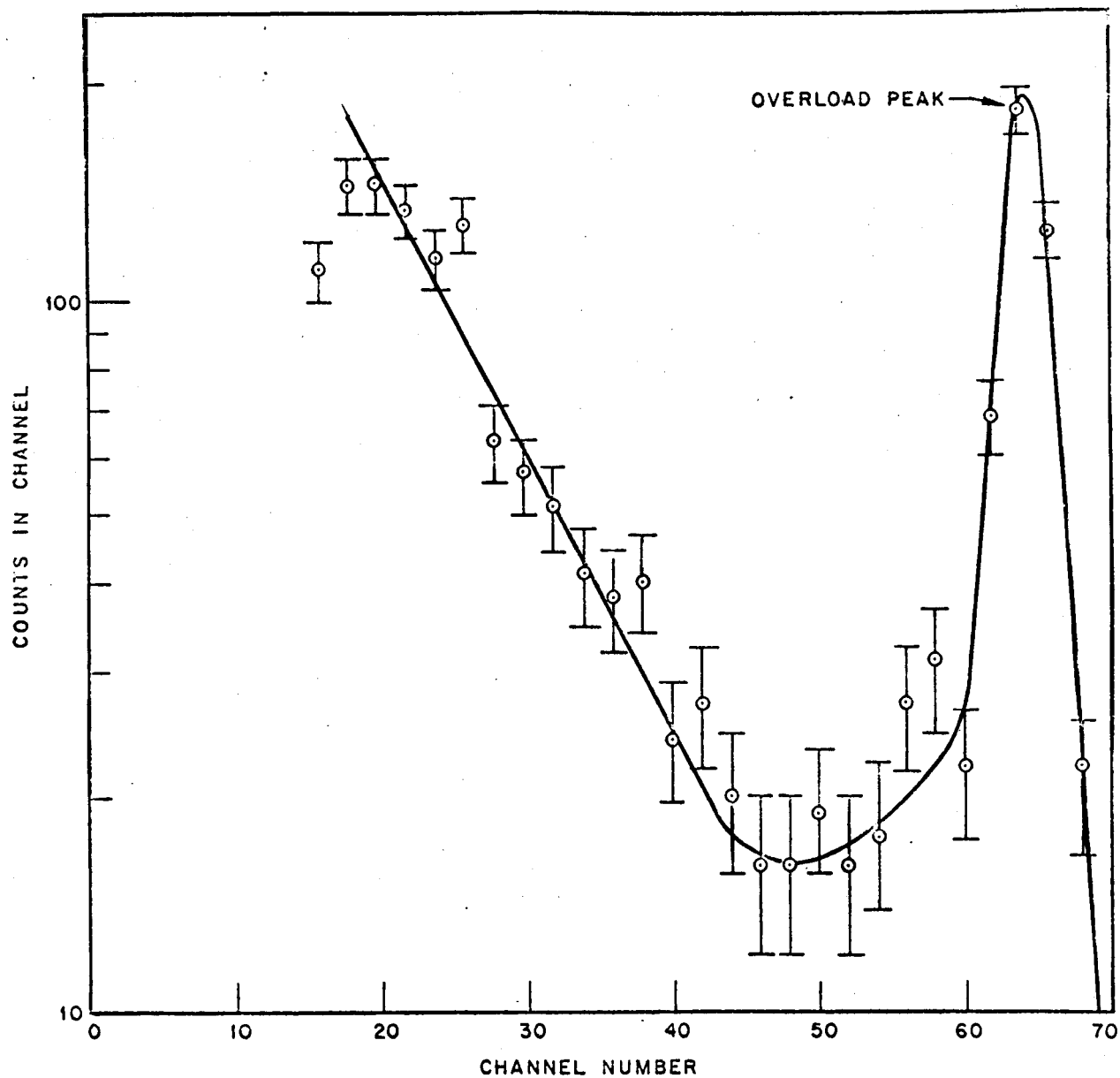


Figure 17. Spectrum Observed in Proton Telescope at Ceiling for Flight 3.

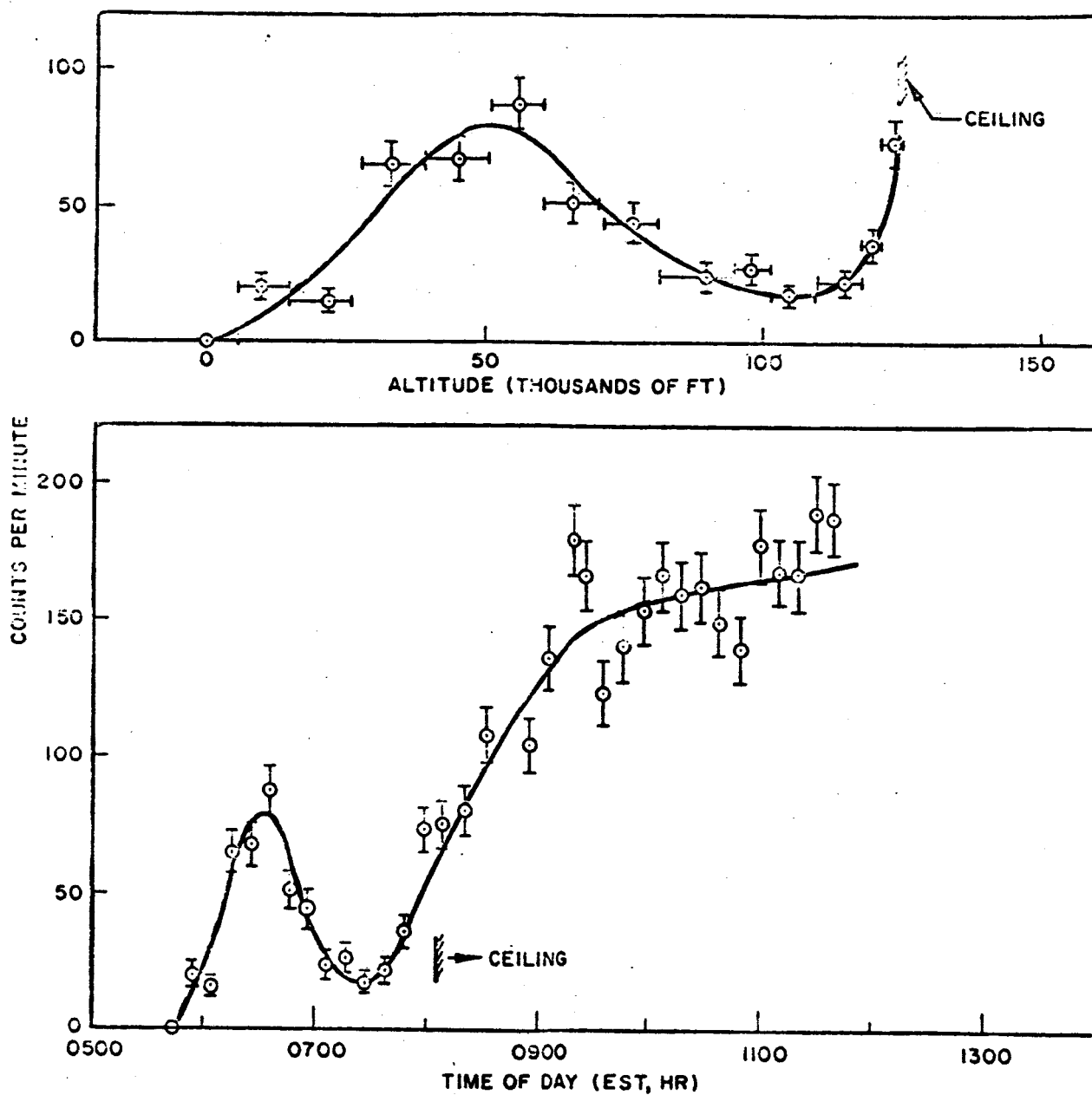


Figure 18. Time and Altitude History of Counting Rate in Proton Telescope for Flight 3.

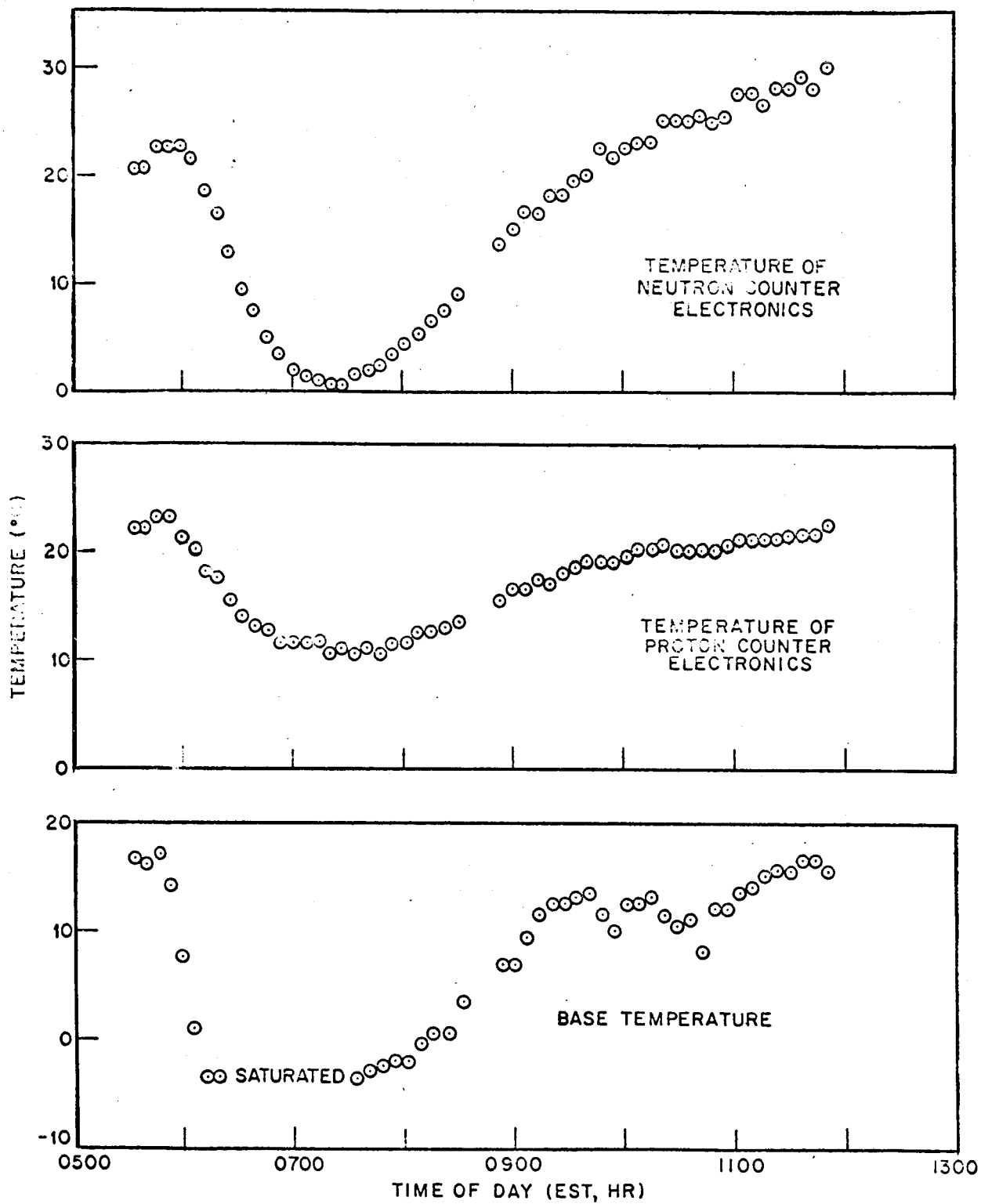


Figure 19. Temperatures Observed During Flight 3.

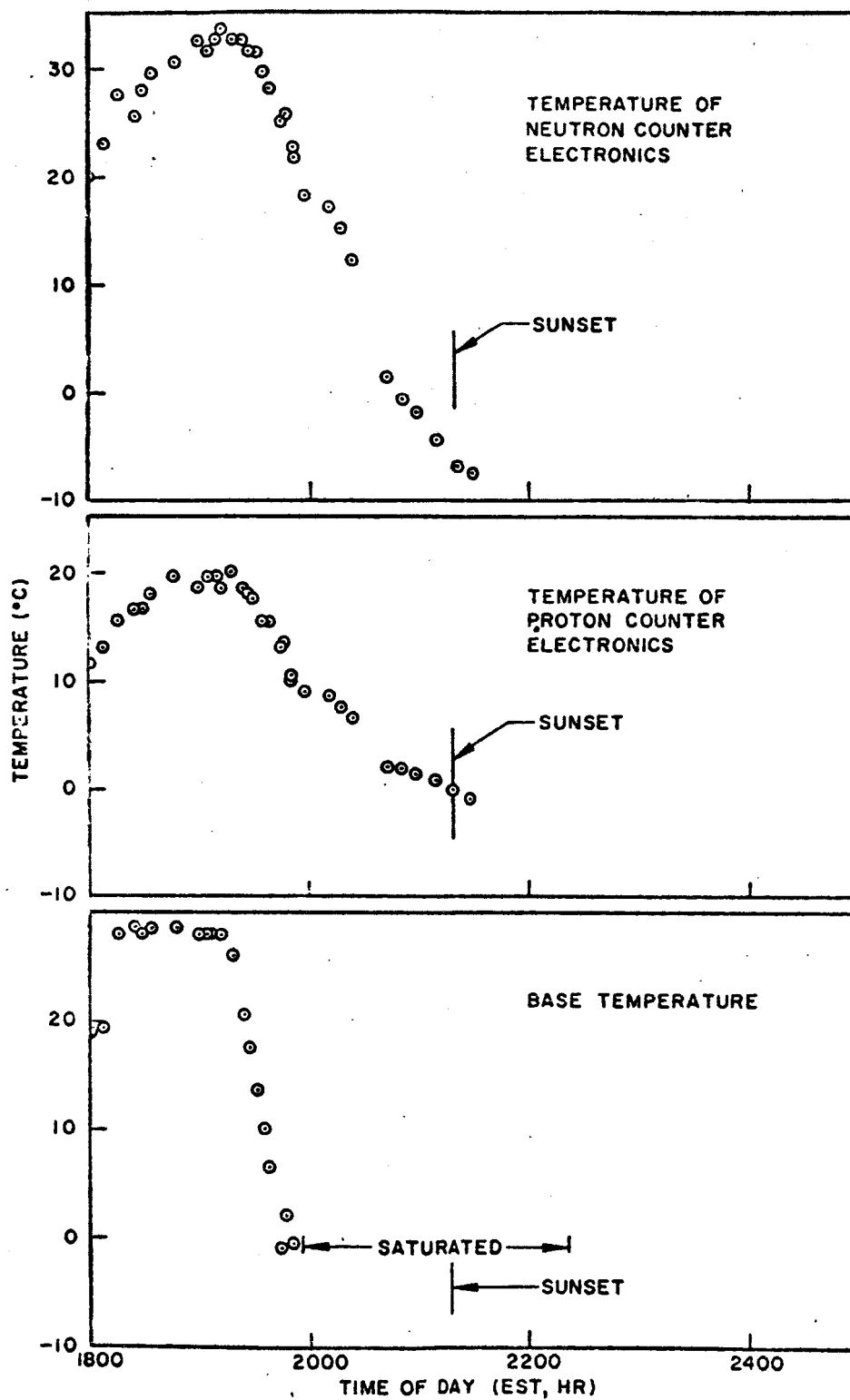


Figure 20. Temperatures Observed During Flight 1.

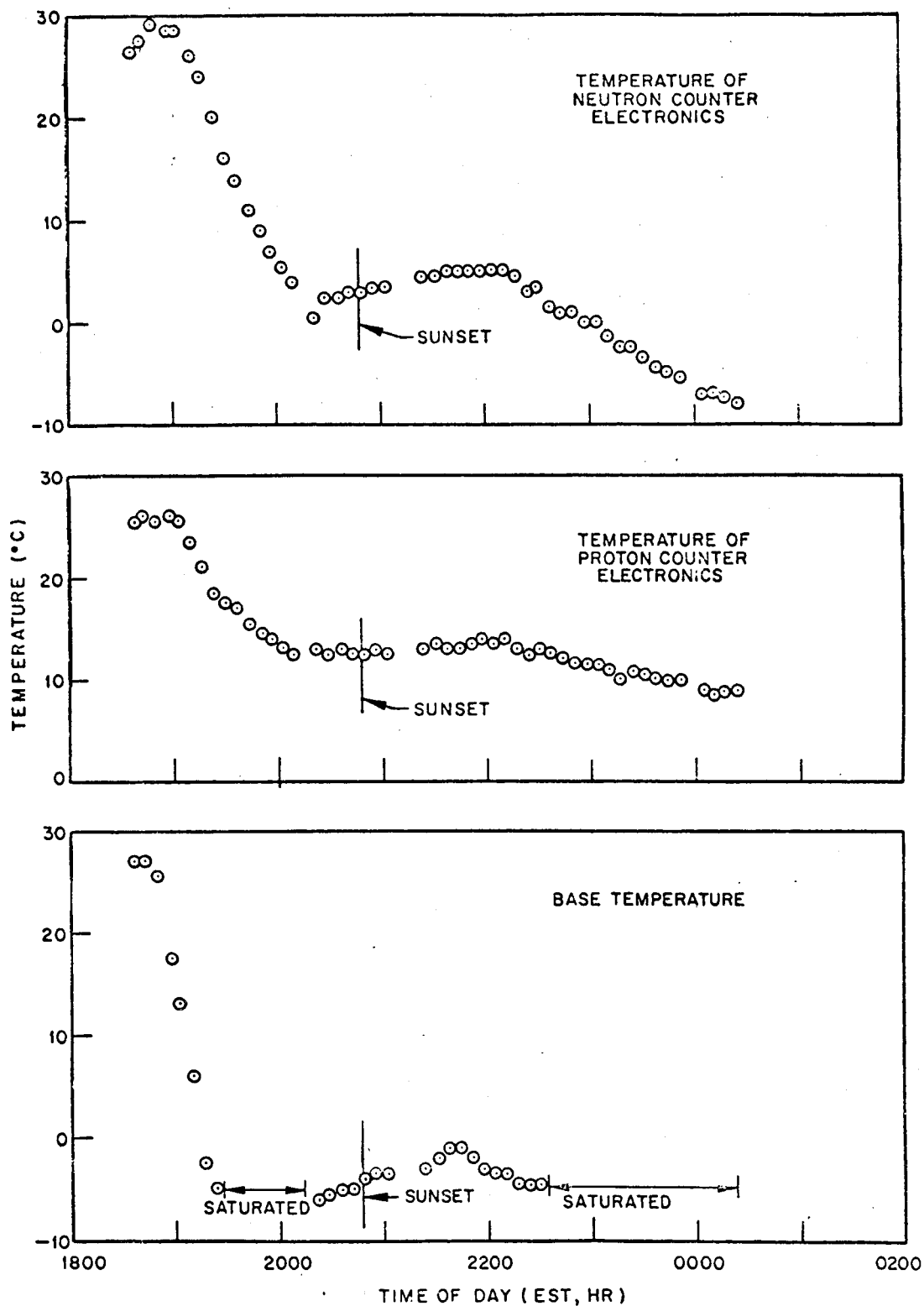


Figure 21. Temperatures Observed During Flight 2.

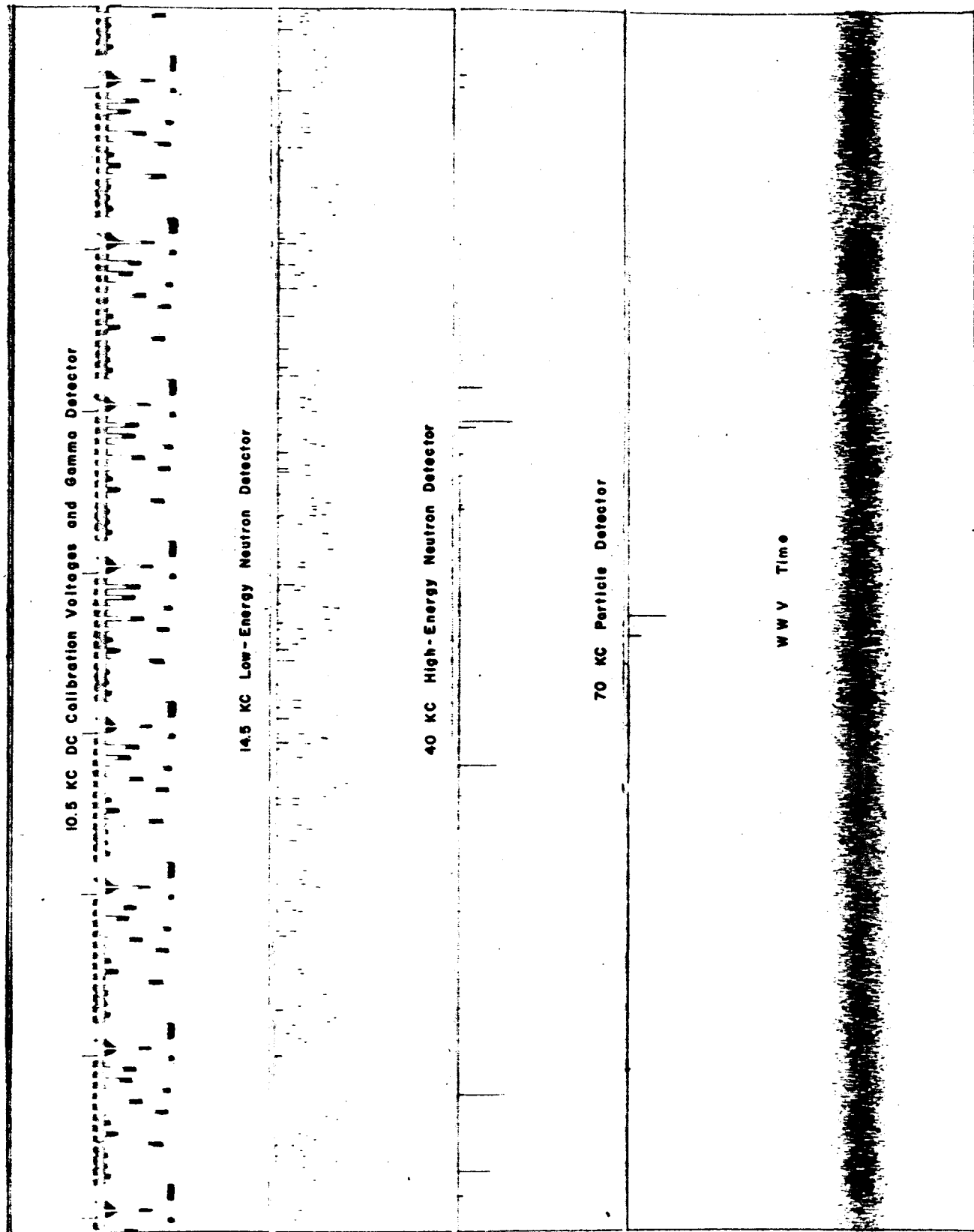


Figure 22. Section of Oscilloscopic Record from Flight 1

IV. CONCLUSIONS

A considerable amount of revising of electronic circuitry and a comprehensive environmental test program are required to improve the reliability of the various detectors.

The neutron counting rates for Flight 1, which took place shortly after a large solar flare, are considerably greater than those for other flights. The rates for the second flight, during which the radiation in the atmosphere was somewhat above normal, are slightly greater than the third flight, for which conditions were normal.

The ratio of counts for the two neutron detectors, A/B, will indicate the relative proportions of high energy and low energy radiation at any altitude. This ratio is nearly the same for the second and third flights and much higher for the first, indicating a considerable increase in high energy neutrons following a solar flare.

V. FUTURE PLANS

The radiation effort of the 6571st Aeromedical Research Laboratory has been limited towards the development of space radiation dosimetry devices. It is also within this area that future efforts lie.

A space radiation monitoring system was completed in June 1962 and is capable of detecting and analyzing impinging radiation, determining the dose rate attributable to the various types of radiation and integrating the total radiation dose rate and total dose. This system was test flown on high altitude balloons during June-July 1962 and it is anticipated that in the future it will be incorporated into space flights.

Also under development is a radiation monitoring system utilizing only solid state detectors. The capabilities of this system are very similar to the one mentioned above; however, complete utilization of solid state detectors and electronics plus microminiaturization of components will result in a smaller, more compact, rugged and lightweight system. It is also designed for space use. Present plans call for its inclusion in space vehicles of different orbital characteristics to enable measurement of the radiation environment in as many different regions of space as possible.

VI. RECOMMENDATIONS

On the balloon flights of 1960 and 1961, the telemetry signal was usually lost by the ground receiving station at the launch site while the balloon was 50 to 100 miles short of the horizon. An additional one to three hours of data could be recorded if a usable signal could be maintained until the balloon passed over the horizon. Additional recording time may be obtained by a few relatively uncomplicated procedures, the simplest of which is to locate the station 100 or more miles down range along the balloon track. For example, a site at Minot or Bismarck, North Dakota would permit 5-1/2 to 8-1/2 additional hours of recording, which is an increase of 60 to 95 percent over the 1960 - 1961 average of 8.9 hours (at altitude). Improvement of the transmitted power to three watts would, according to calculations, increase the range to the horizon. If 19 cells were used in the battery pack, the average voltage would be 29 volts, which would provide exactly three watts (Table II, App. B) over 90 percent of the pack life. This assumes that the transmitter is carefully tuned to its antenna. As noted in Appendix B, additional cells decrease the transmission time. However, the 18 hours available with 19 cells would be adequate for a balloon to cross the horizon at speeds as low as 28 mph. During the 1960 - 1961 flights, the lowest speed encountered was 33 mph. Acceptable signal reception in the ground station was maintained by careful attention to such details as the use of cables of the correct impedance and frequent performance checks of preamplifier and receivers to assure that they meet the manufacturer's specifications.

REFERENCES

1. Wallner, Lewis E., Harold R. Kaufman, "Radiation Shielding for Manned Space Flight," NASA TN D-681.
2. Anderson, Kinsey A., "Preliminary Study of Prediction Aspects of Solar Cosmic Ray Events," NASA TN D-700.
3. Simons, D. G., "Stratosphere Balloon Techniques for Exposing Living Specimens to Primary Cosmic Ray Particles," TR 54-16 Holloman Air Force Base, New Mexico.

APPENDIX A

RADIATION DETECTION SYSTEM CIRCUITRY

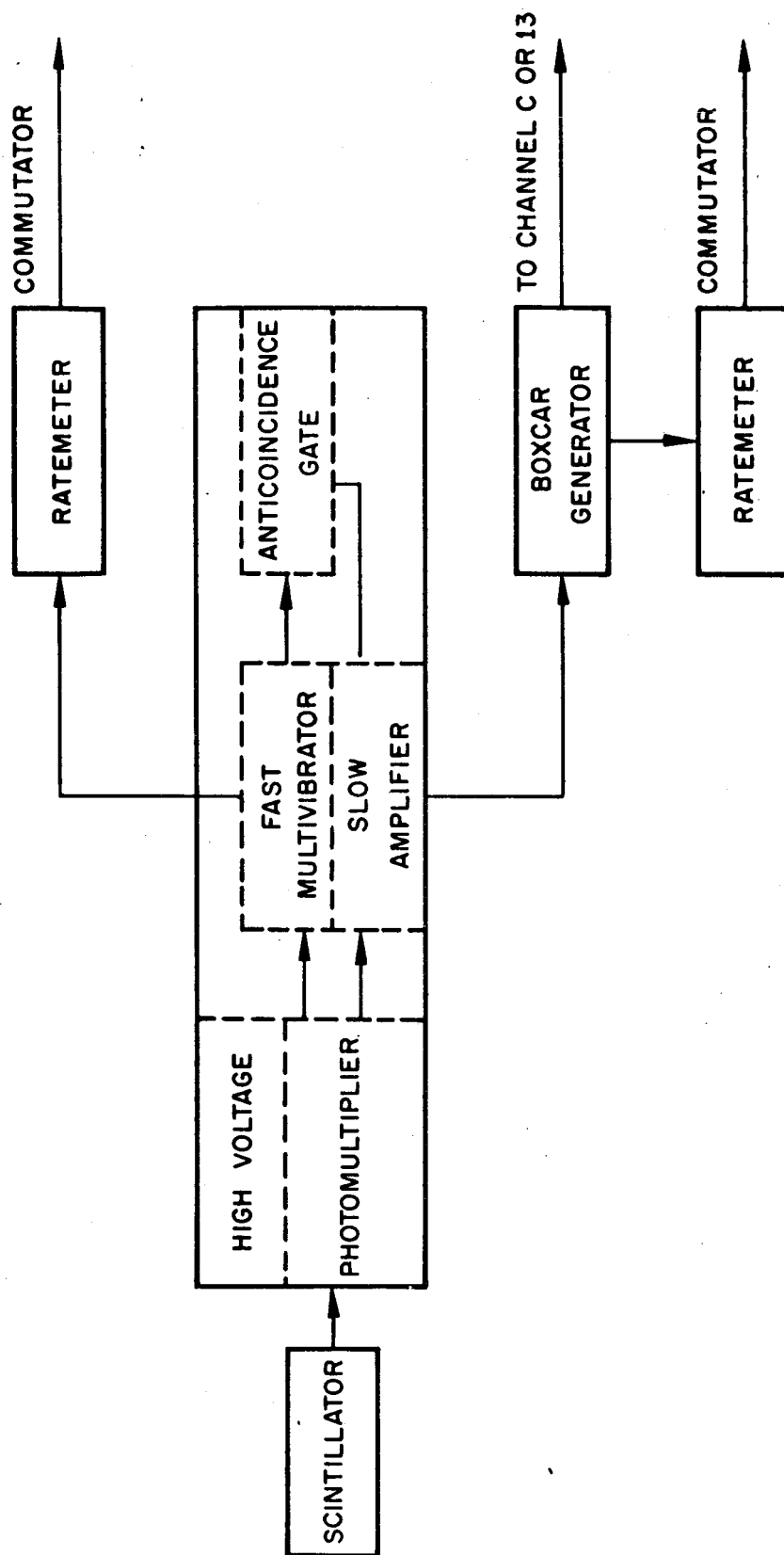


Figure 23. Block Diagram of Neutron Detector Electronics

7151 PHOTOMULTIPLIER

PIN NO.

12

1

11

2

10

3

9

4

8

5

7

6

HIGH-VOLTAGE
POWER
SUPPLY

MODEL
3GA

+ 28 V

GROUND

A
B

J-1
PC02P-8-2P

R-1
2K

D-1
IN936A

+ C-1
1MFD.

J-2
MICRODOT
31-50
SIGNAL OUTPUT

RG-174/U
AMPHENOL
21-598

R-2
10K

R-5
20K

R-6
20K

C-2
1MFD.

C-3
1MFD.

TR-1
2N501A

TR-2
2N501A

D-3
IN906

R-4 5.1K

R-3
51K

D-2
IN906

Figure 24. Photomultiplier Detector for Proton Telescope



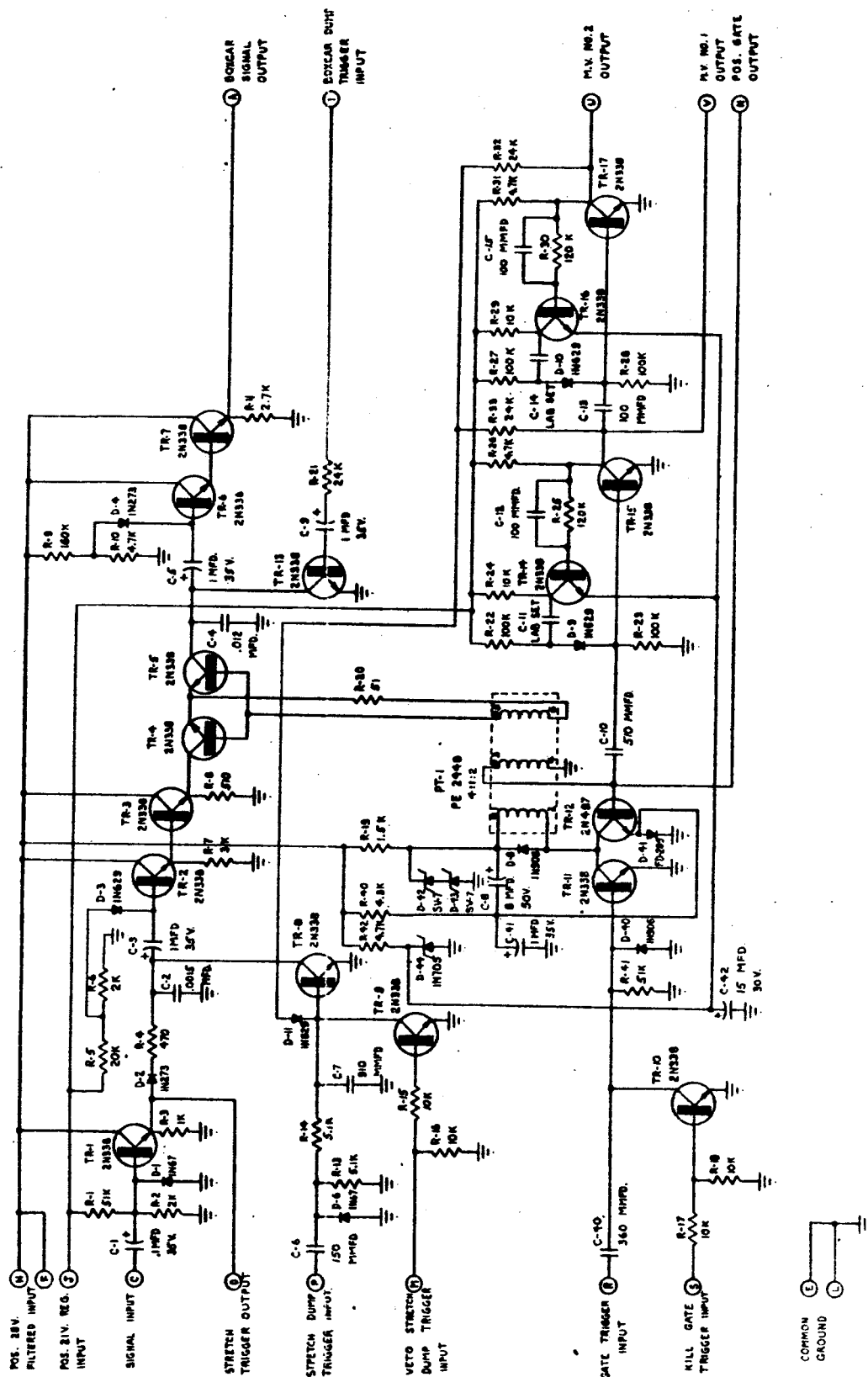


Figure 26. Boxcar Run-down Generator

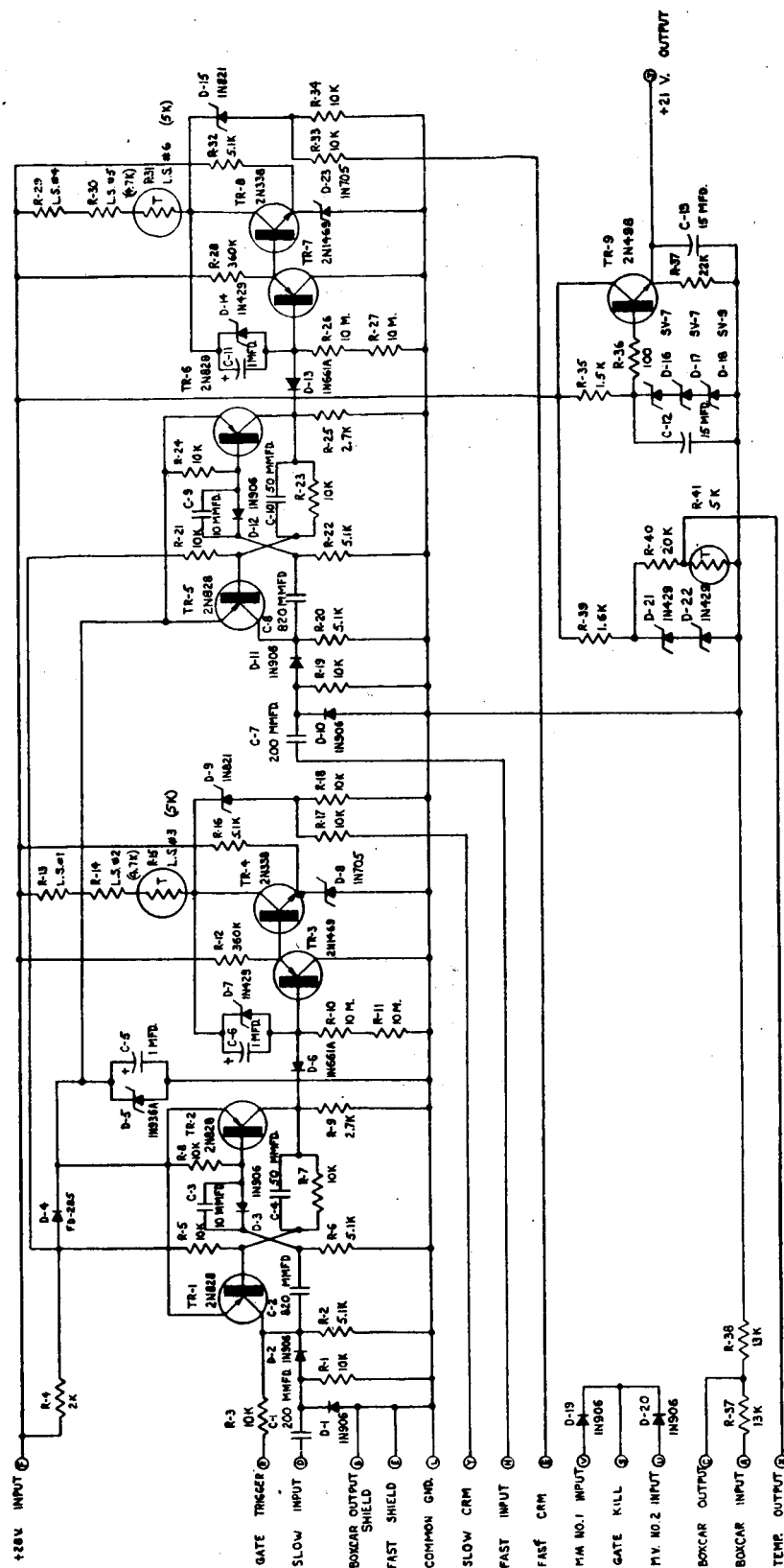


Figure 27. Phoswich Count Rate Meter

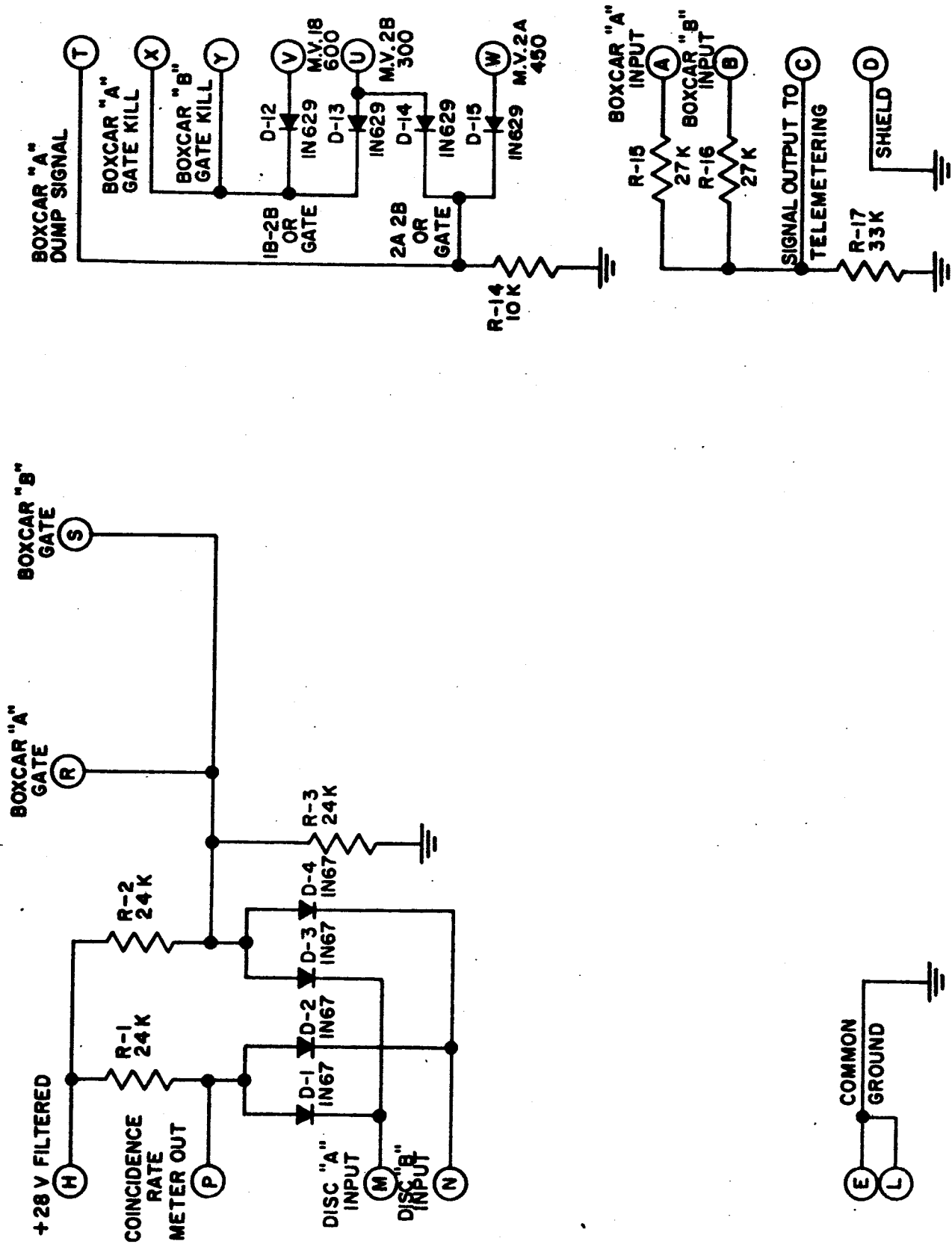


Figure 28. Telescope Logic Circuit Board 3

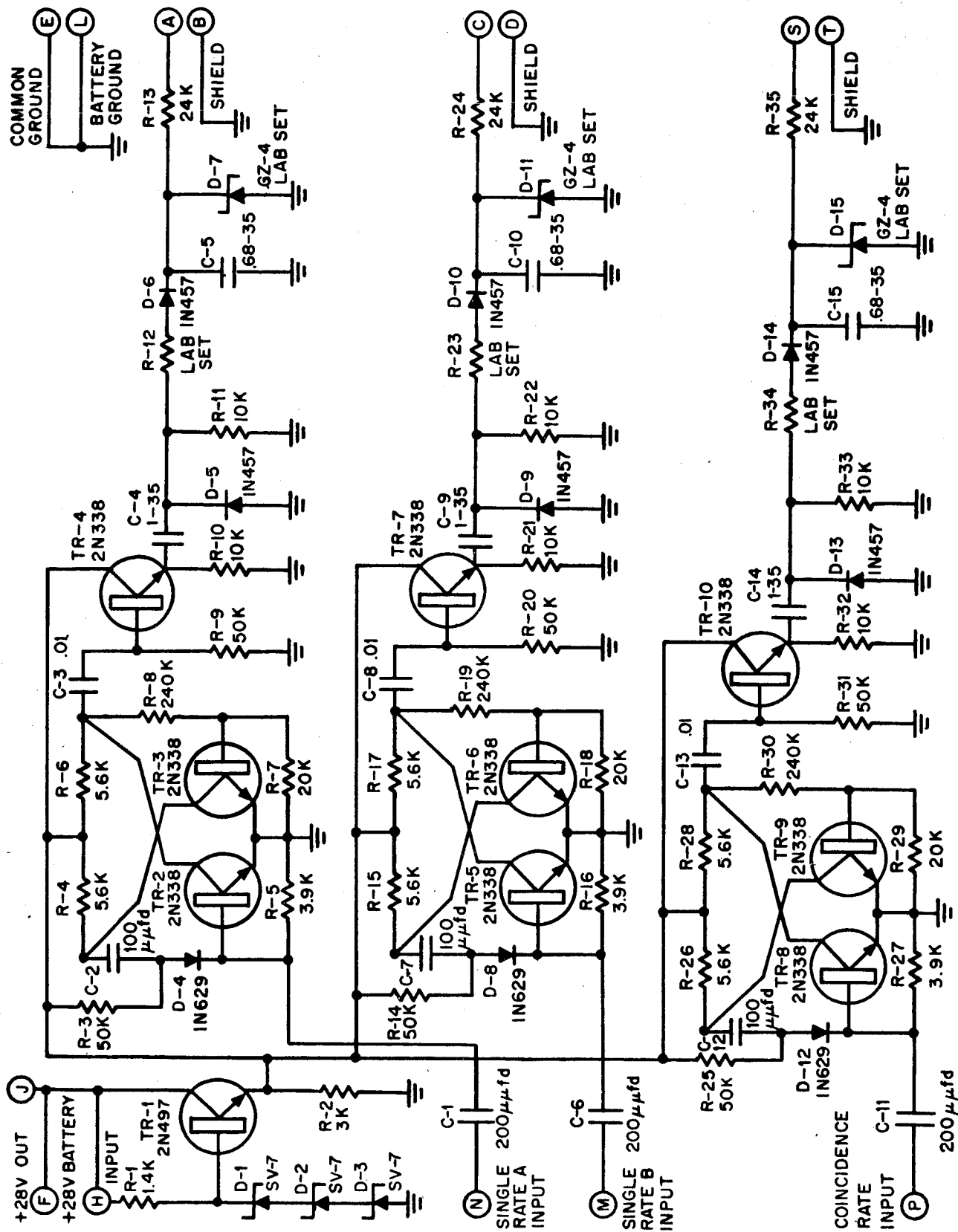


Figure 29. Count Rate Meters Board 4

APPENDIX B

DETAILED DISCUSSION OF DATA ACQUISITION EQUIPMENT AND PROCEDURES

I. EQUIPMENT USED

The transmission system was the same one used the previous year; a Dorsett TMS-106L tube type two-watt transmitter and ten subcarrier oscillators covering IRIG channels 6 through 13 plus C and E. The system is shown in Figure 30 with the transmitter at the upper right. The three screwdriver adjustments on top of each oscillator, control the band edge frequencies and the output voltage. The package was bolted to the cover of an aluminum box which housed the battery pack used to power the transmitter (Fig. 31). Signal output leads from the radiation detection packages were attached to the terminal board on the end of the box, from which a cable ran to the telemetry system input (Fig. 32). The transmission antenna (Fig. 33) was an Andrew "discone" type with unity gain, which was tied to the balloon payload with nylon cord in such a manner that it hung below everything in the flight train. Connection to the transmitter was made with a four foot length of RG-58/U coaxial cable. The antennas were invariably damaged beyond repair when the payload hit the ground, so a new one was required for each flight. A complete spare transmission system with power pack was maintained in readiness in case the main unit was lost or damaged.

The transmitter was powered by a block of 17 silver-zinc cells completely surrounded by styrofoam in the battery box (Fig. 31). The average voltage provided was 25 volts at 3.1 amperes. The two sets of cells were new and were obtained from the manufacturer fully charged, but containing no electrolyte. At the launch site, the potassium hydroxide solution was pumped into the cells by individual squeeze bottles. They were allowed to stand 72 hours to build up capacity and then assembled into packs of 17 cells.

The length of time the battery pack will operate the telemetry transmission system at a practical level of power output may be determined from a graph supplied by the manufacturer of the cells and the data in Table II. The Yardney Electric Corporation booklet on "Silvercel" silver-zinc cells (dated 1960) contains a plot of percent of nominal capacity vs. cell voltage, which shows the drop from full charge to the plateau or constant voltage and the rapid drop off when the cell is near exhaustion.

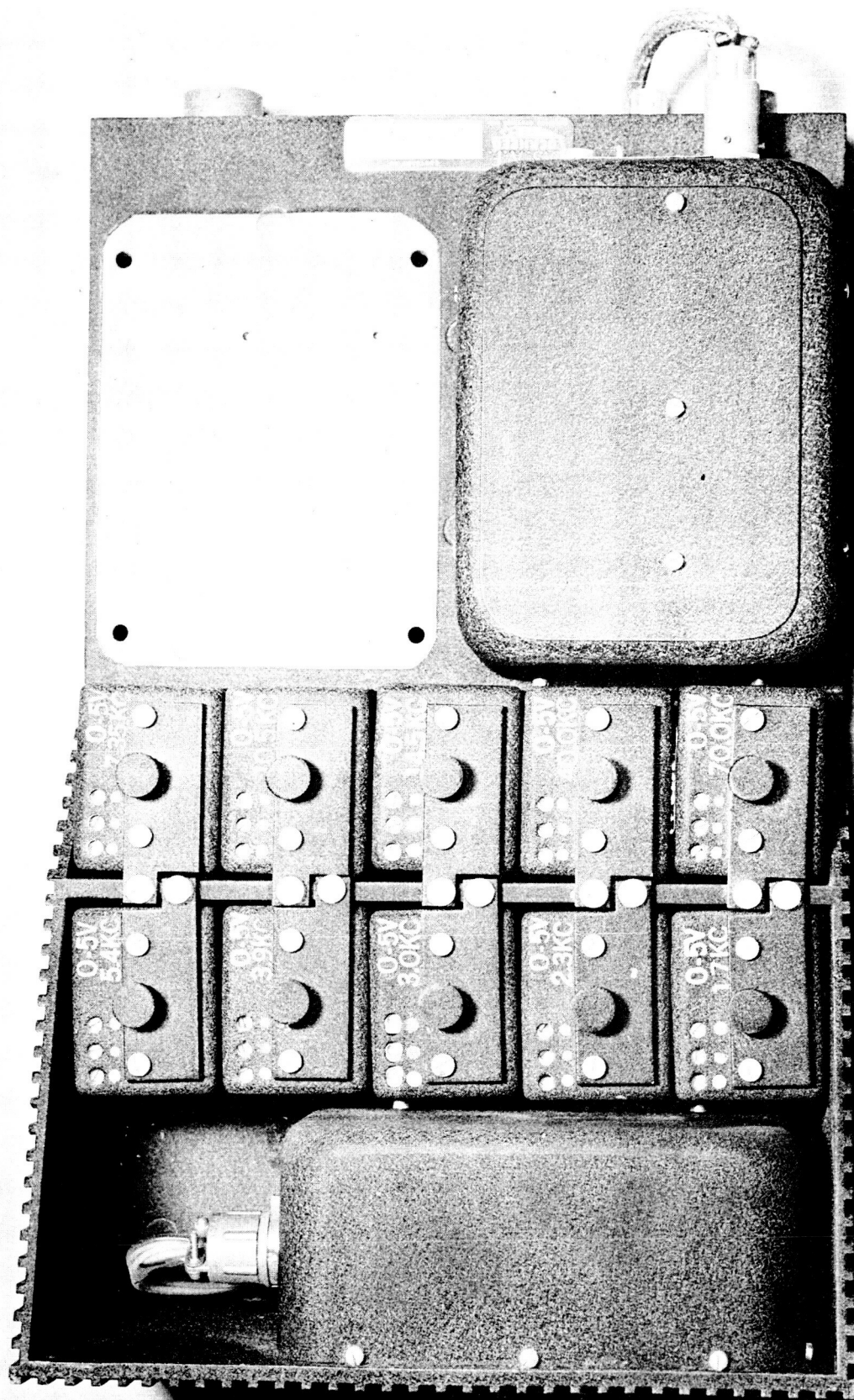


Figure 30. Top View of Telemetry Transmission System

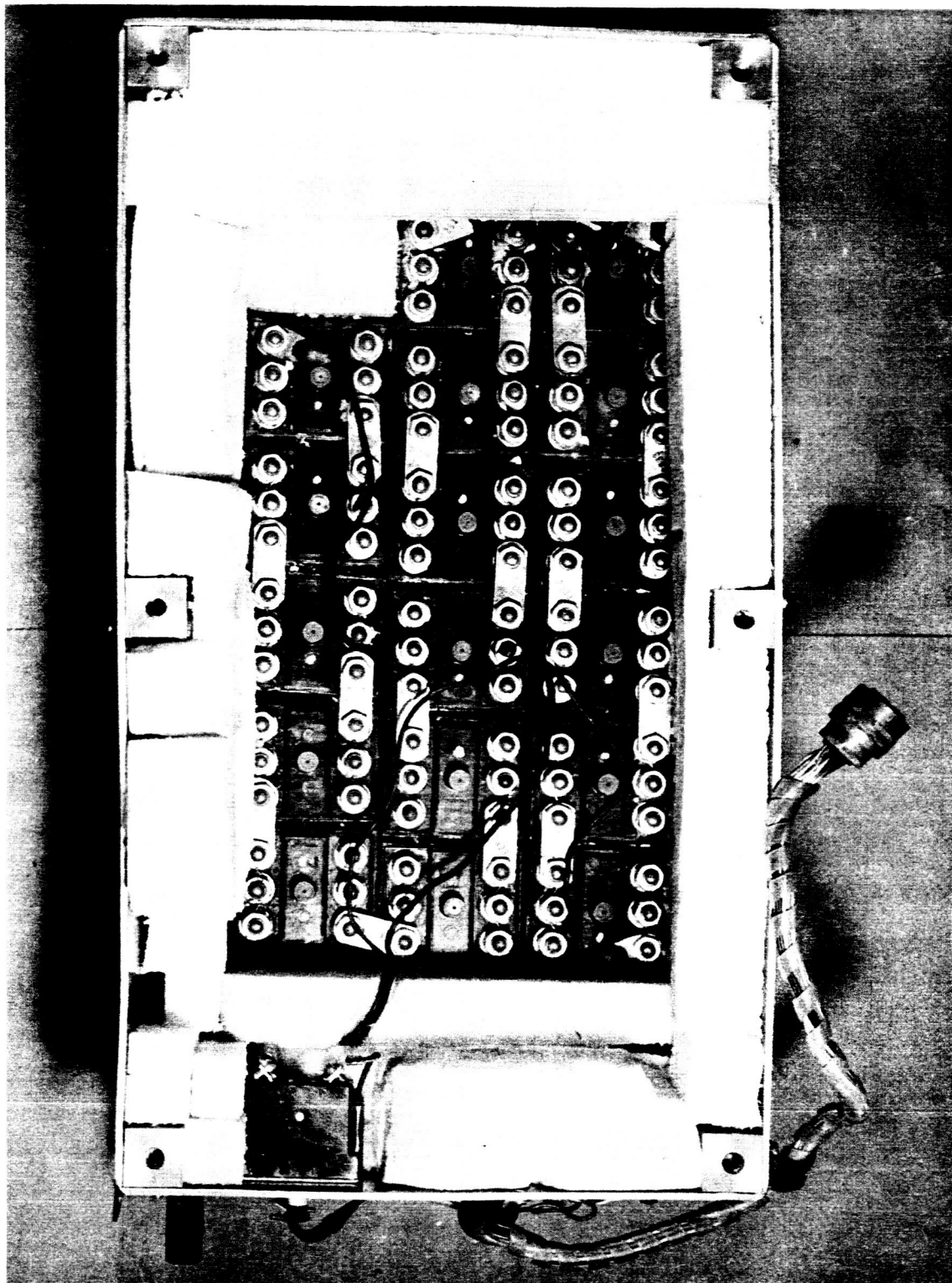


Figure 31. Top View of Battery Box

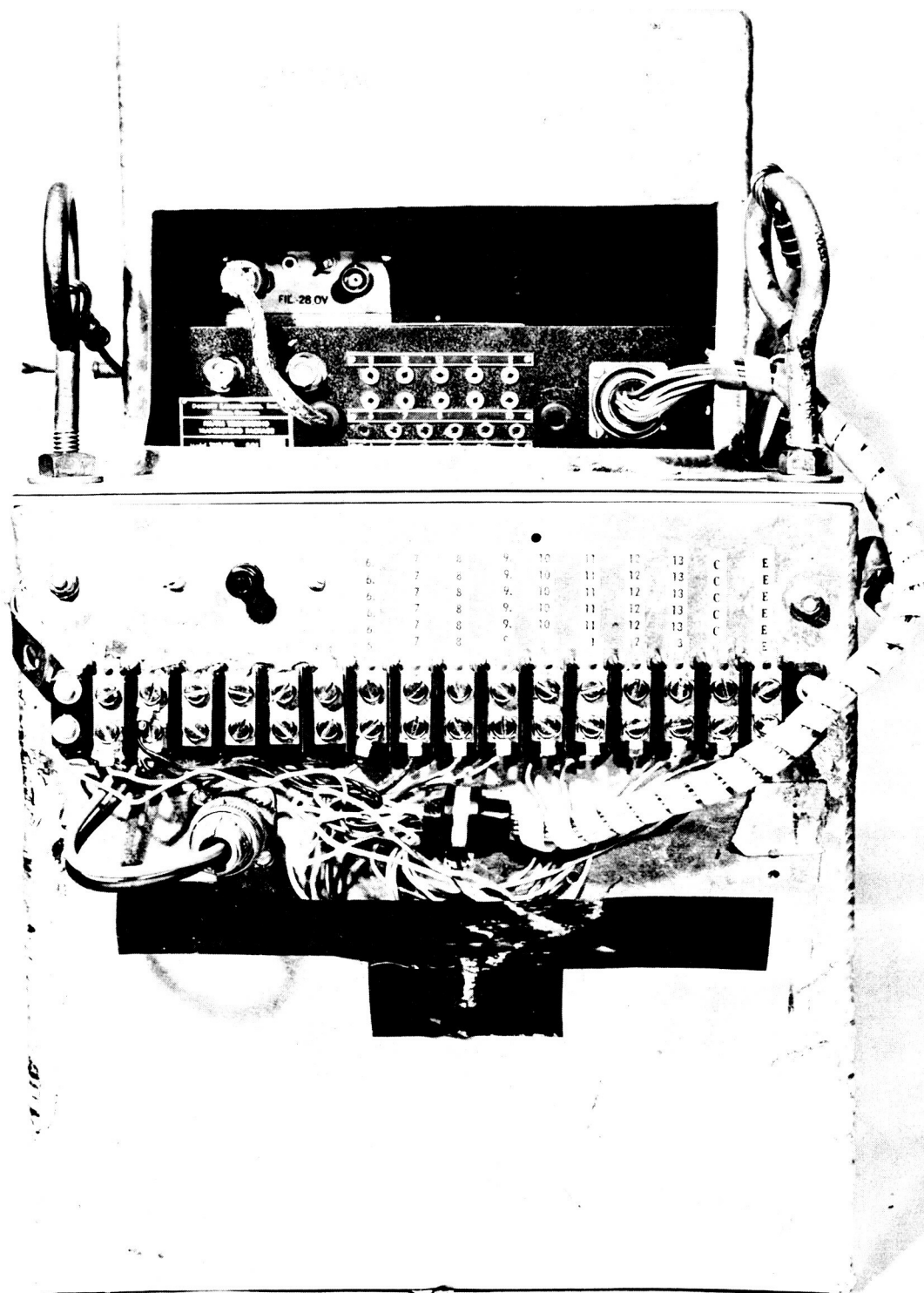


Figure 32. Signal Input Strip on End of Battery Box

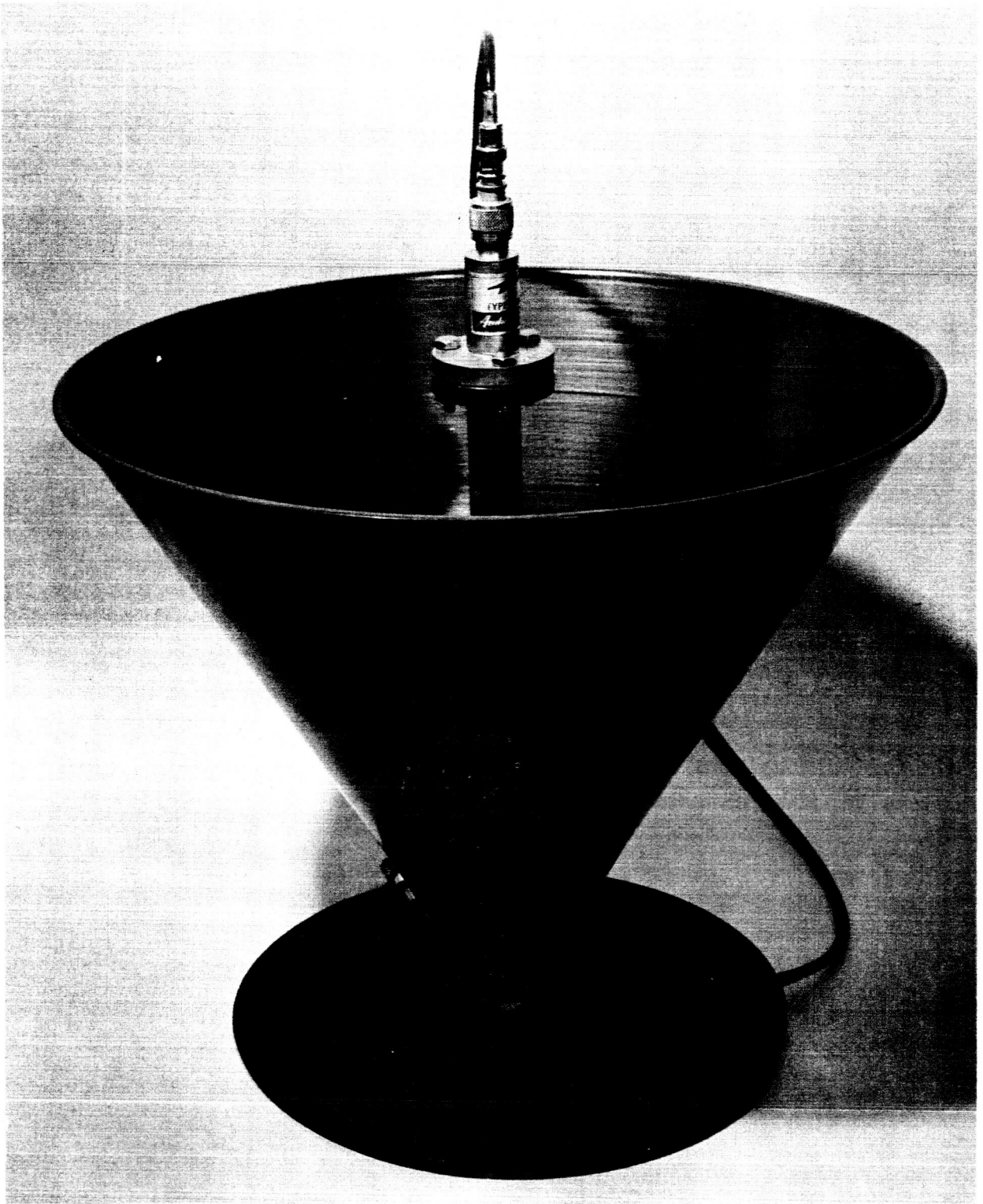


Figure 33. Telemetry Transmission Antenna

If the percentages of nominal capacity at the end of the plateau just before rapid drop off are plotted against the rates of discharge of the cells, it will be observed that at a 20 hour discharge rate, 123 percent or 74 ampere-hours may be drawn from the nominal 60 ampere hour cells used on these flights. To this may be added the additional capacity available while the voltage is decreasing to its lowest usable value (empirically, this is 22 volts for the battery pack). Since the input to the telemetry transmission system should not exceed 30 volts, the battery pack must be adjusted to this value before the start of a flight. Depending upon the number of cells in the pack, a certain percentage of nominal capacity will be lost through this adjustment and must be eliminated from the total. The values of ampere hours for each segment of the curve may be divided by the average current over that voltage range (from Table II) to obtain the number of hours of signal transmission. With a 17-cell battery pack, the voltage will change from 30 to 22 in 23 hours. The addition of one cell to the pack will decrease the time to 20 hours, and two cells will permit operation for 18 hours.

The ground receiving station was mounted in a small van which was completely self contained except for a power cable. At the launch site (Bemidji Airport), it was parked outside the work building with the cable running through the building wall to a power distribution box. The telemetry receiving antenna, a bifilar or double eight-turn helix with a specified gain of 14 db, was mounted on a tripod on the van roof (Fig. 34). It could be rotated through 360 degrees and tilted from below the horizon almost to the zenith. The incoming signals were routed through the antenna to a preamplifier and the telemetry receiver. From there they were recorded and monitored as shown on the block diagram of the ground station (Fig. 35). The layout of the van is shown in Figure 36, and pictures of the instrument cabinets are shown in Figures 37, 38, and 39. Because of the increase in instrumentation over the previous year, more rack space was required, and the cabinets had to be mounted against the walls, leaving a center aisle. To facilitate cabling and other work behind the cabinets, the tape recorder was pulled away from the wall as far as practical and the others were rolled out on casters. For travelling, all cabinets were bolted to the van floor and wall. No damage to any equipment was observed as a result of the 3000 mile trip. Most of the instruments and equipment not mounted in the cabinets were contained on several storage shelves at the front of the van. They were provided with sliding doors to prevent spillage while driving. At the rear of the van were two additional storage shelves with a fold-down cover to protect the contents. When the cover was put up and supported

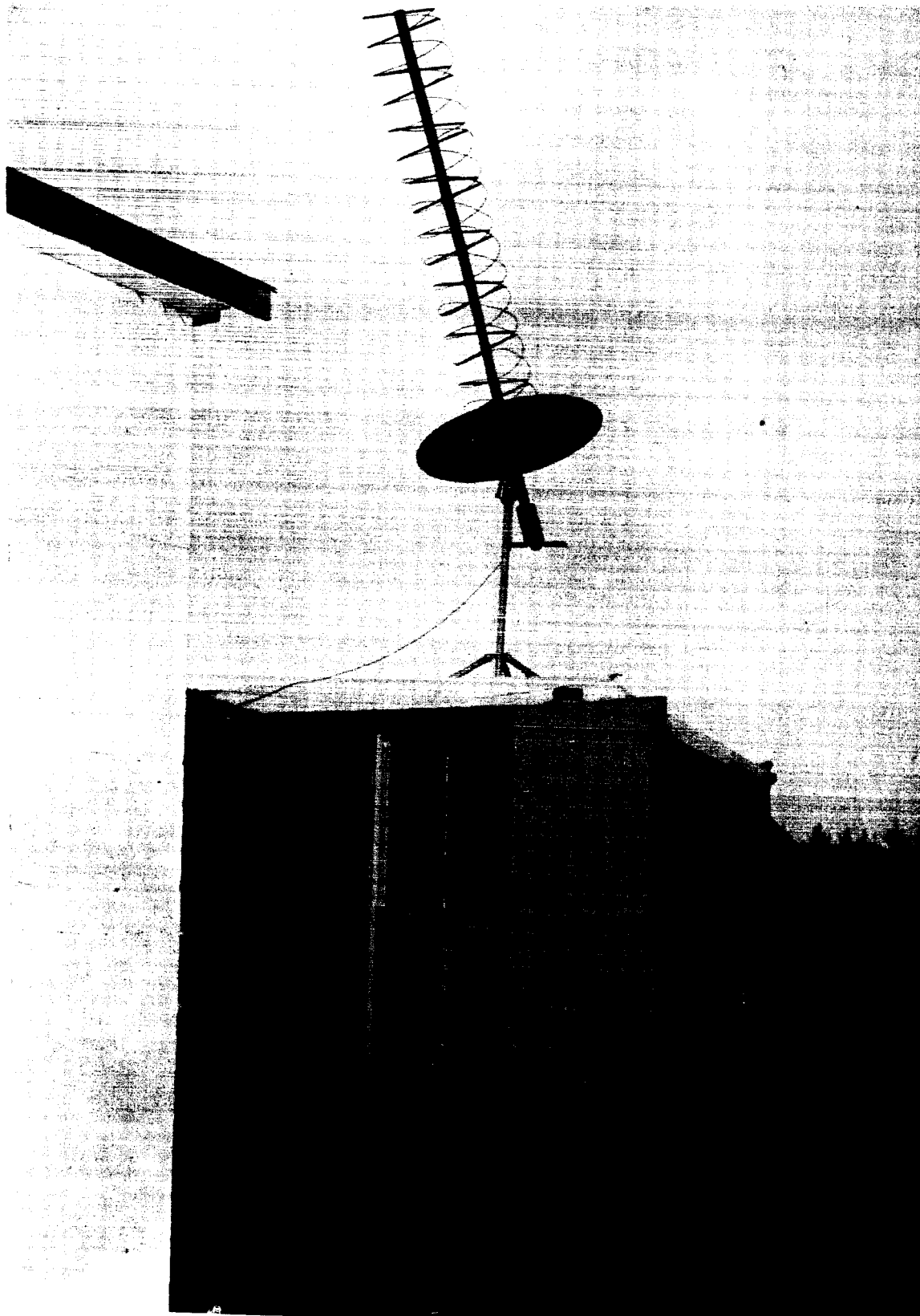


Figure 34. Telemetry Van

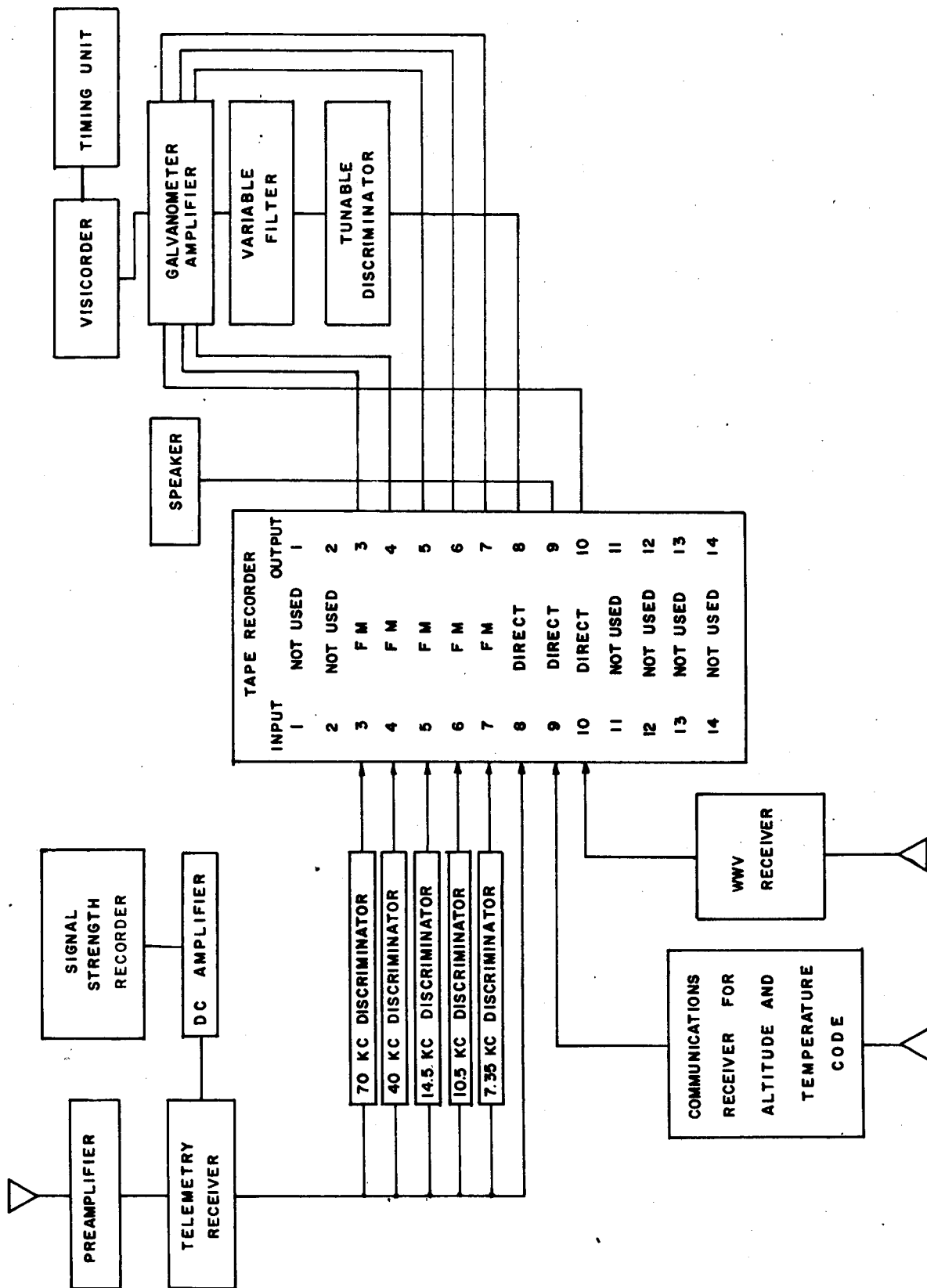


Figure 35. Block Diagram of Ground Receiving Station

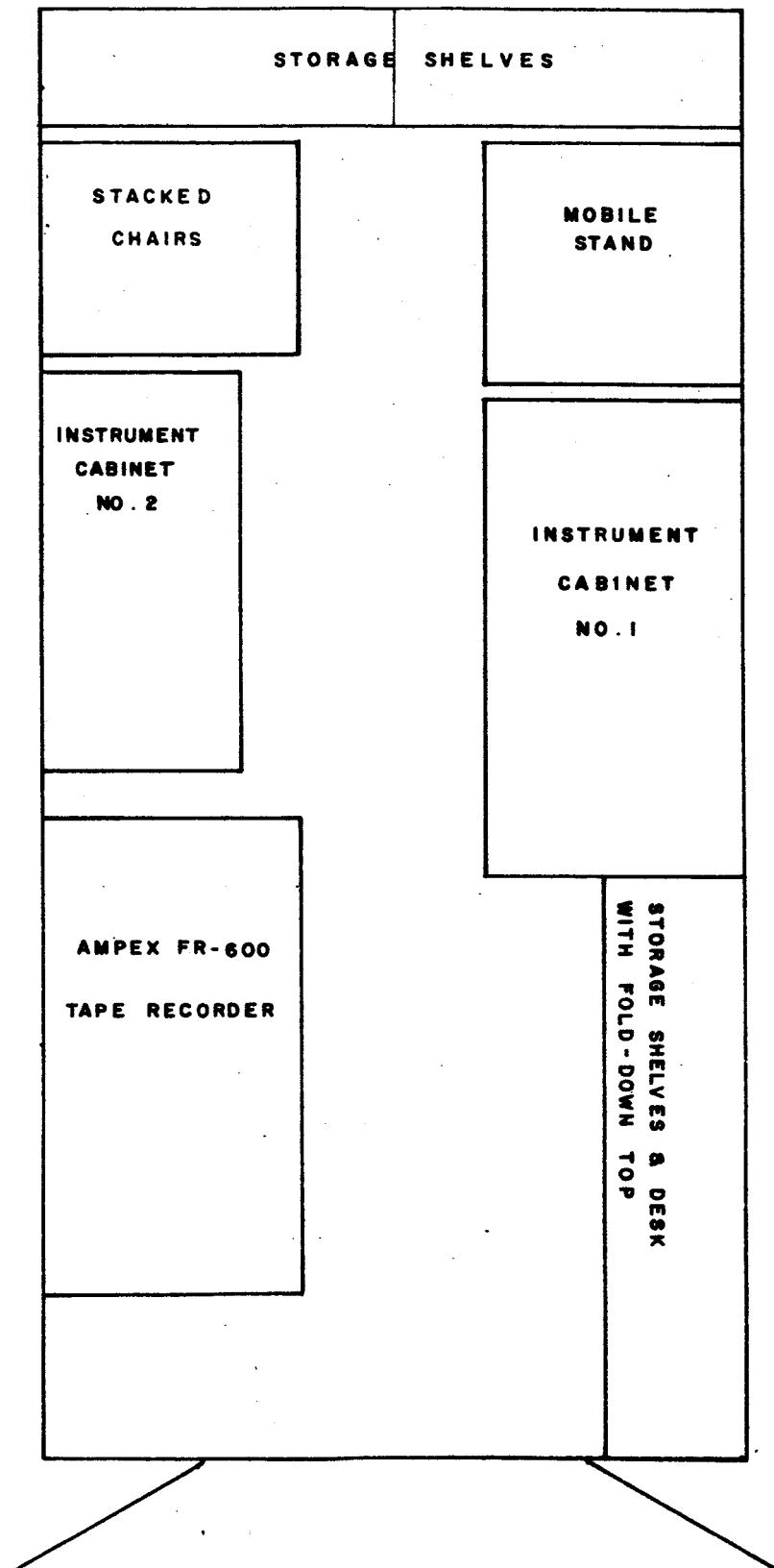


Figure 36. Layout of Telemetry Van

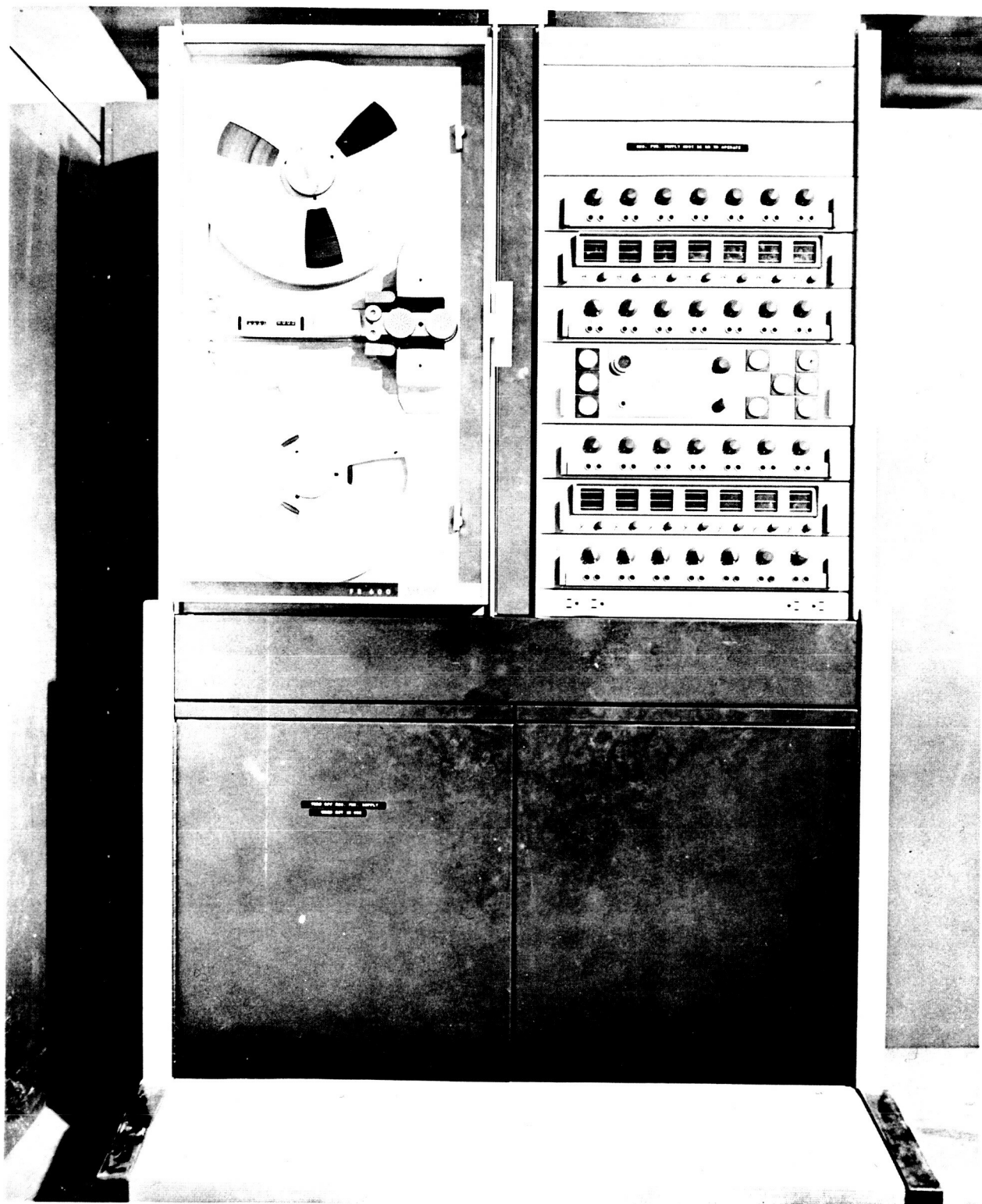


Figure 37. Tape Recorder

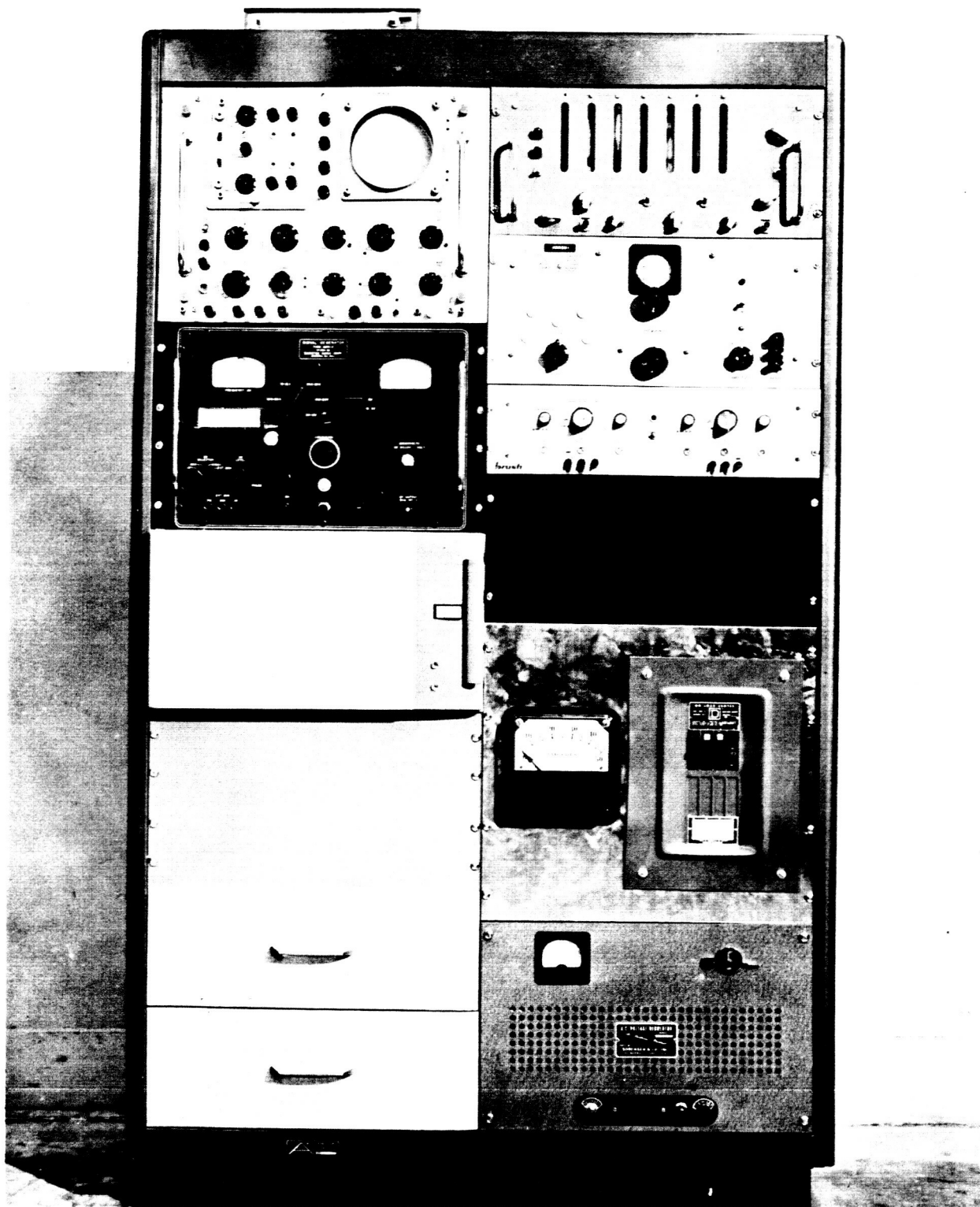


Figure 38. Cabinet 1, Telemetry Ground Station

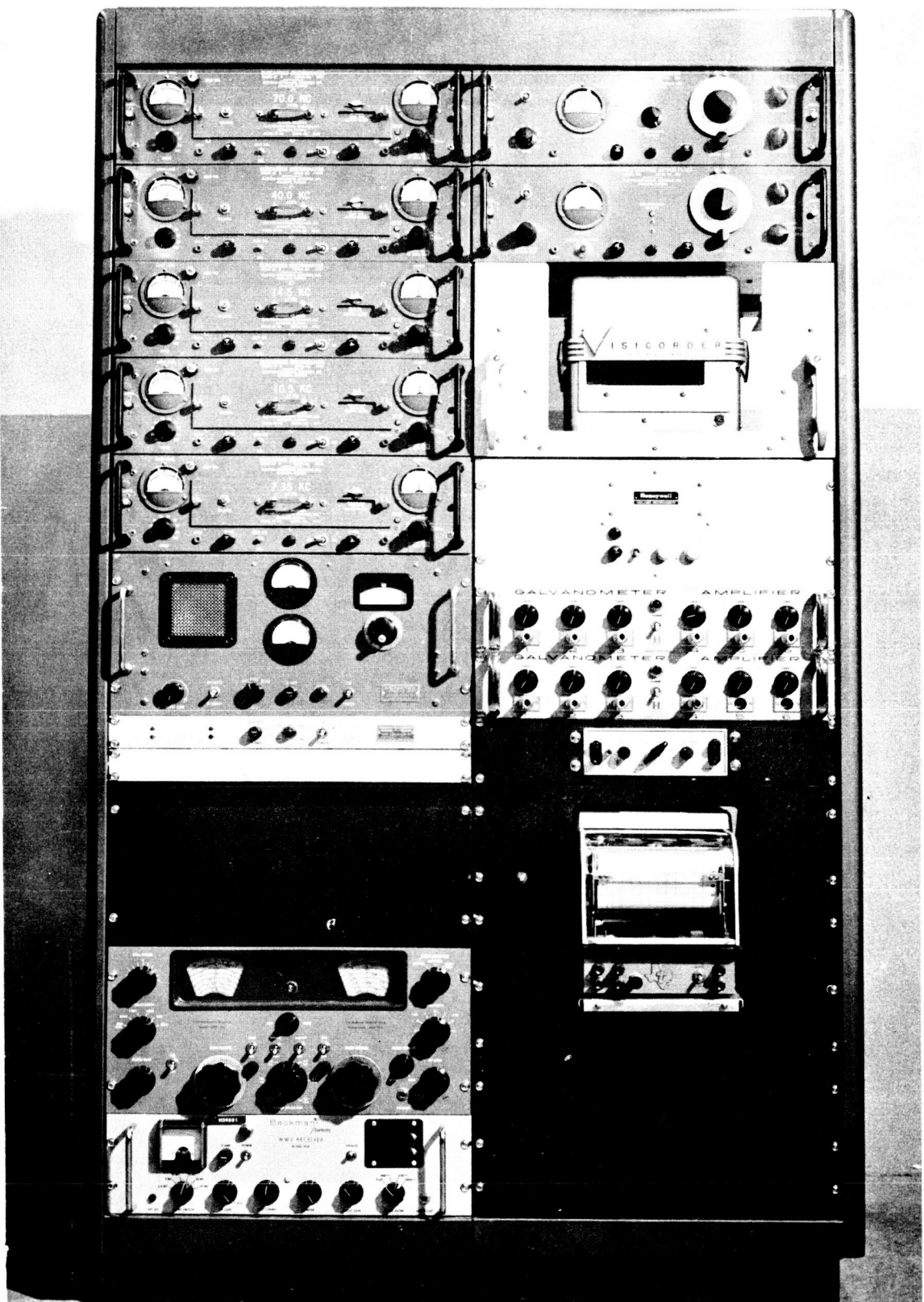


Figure 39. Cabinet 2, Telemetry Ground Station

on legs, it formed a 3-inch by 5-inch working surface. Equipment cooling was accomplished by several small fans and a room type air conditioner, which was quite inadequate for the job. The tape recorder and discriminators developed considerable heat. A list of instrumentation used in the ground station may be found in Table III, while the monitoring and test equipment is listed in Table IV.

TABLE II

TRANSMITTER CHARACTERISTICS WITH VARIOUS
OPERATING VOLTAGES, DORSETT TYPE TMS-106L SYSTEM,
SERIAL NUMBER 120, USED ON ALL FLIGHTS

| <u>Input VDC</u> | <u>Current Amps</u> | <u>Power Out Watts</u> |
|----------------------|-------------------------|----------------------------|
| 22 | 2.8 | 1.4 |
| 23 | 2.9 | 1.6 |
| 24 | 3.0 | 1.8 |
| 25 | 3.1 | 2.1 |
| 26 | 3.2 | 2.3 |
| 27 | 3.4 | 2.6 |
| 28 | 3.6 | 2.8 |
| 29 | 3.7 | 3.0 |
| 30 | 3.9 | 3.2 |

TABLE III
GROUND RECEIVING STATION EQUIPMENT

| <u>Item</u> | <u>Manufacturer and Model</u> |
|--|--------------------------------------|
| Antenna, helical, bifilar | Andrew Model 52000-2 |
| Preamplifier for telemetry receiver | Nems Clarke Model PR-203 |
| Receiver, telemetry | Nems Clarke Model 1670 G |
| Recorder, strip chart, DC | Texas Instruments Recti-Riter |
| Amplifier, DC | Texas Instruments Model 301 |
| Discriminators (5), 7.35, 10.5, 14.5, 40 and 70 kc | ElectroMechanical Research Model 67D |
| Receiver, communications | Technical Materiel Model GRP-90 |
| Receiver, WWV | Beckman/Berkeley Model 905 |
| Recorder, magnetic tape | Ampex Type FR-600 |
| Discriminator, tunable | ElectroMechanical Research 97D |
| Filter, variable | ElectroMechanical Research Model 95D |
| Amplifier, galvanometer (2) | Honeywell Model T6GA |
| Recorder, oscillographic | Honeywell Model 906B Visicorder |
| Speaker, wall baffle | Utah Model DM8-A |
| Regulator, line voltage | Sorensen Model 2000 S |
| Degausser, magnetic tape | Ampex Model SE-10 |
| Cabinet, two section (2) | AMCO Engineering Co |

TABLE IV
MONITORING AND TEST EQUIPMENT

| <u>Item</u> | <u>Manufacturer and Model</u> |
|---|-------------------------------|
| Voltmeter, vacuum tube | Hewlett Packard Model 400H |
| Voltmeter, differential | Fluke Model 803 |
| Oscilloscope, portable battery operated | Tektronix Model 321 |
| Micro-ammeter, volt ohm | Simpson Model 269 |
| Wattmeter, RF | Bird Model 1306 |
| Oscilloscope, rack mounting | Tektronix Model RM-45A |
| Generator, signal | Boonton Model 225A |
| Counter, electronic | Berkeley Model 7360 |
| Oscillator, telemetry checking | Hewlett Packard Model 200TR |

The airborne receiving station was designed to be an emergency backup for the ground station and to record data after the balloon had drifted beyond the range of the ground station. It was housed in a C-123 type aircraft (Fig. 40) and powered by four specially installed 60 cycle inverters. It consisted of a 250 MC stub antenna, telemetry receiver and a 7-track tape recorder on which the composite signal was directly recorded. To permit operation of the recorder at an economical tape speed (15 inches/second), IRIG channels C and E were discriminated and separately recorded on two other tracks. Voice commentary and WWV time were also recorded. Monitoring of the data was accomplished by a dual channel oscilloscope and a speaker. A block diagram of the airborne station is presented in Figure 41, and the equipment is illustrated in Figure 42. A list of the components may be found in Table V.



Figure 40. Air Force Tracking Aircraft

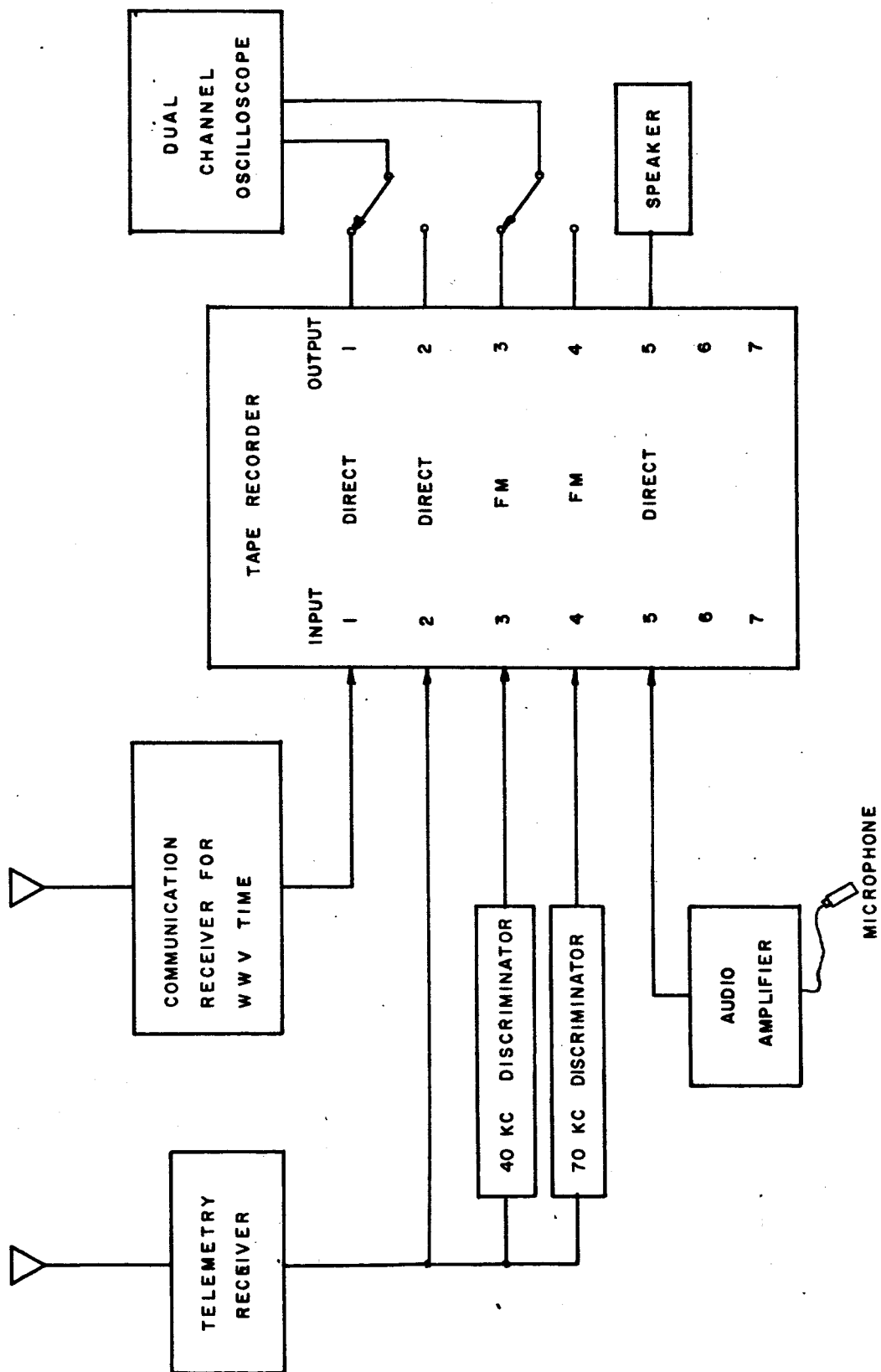


Figure 41. Block Diagram of Airborne Receiving Station

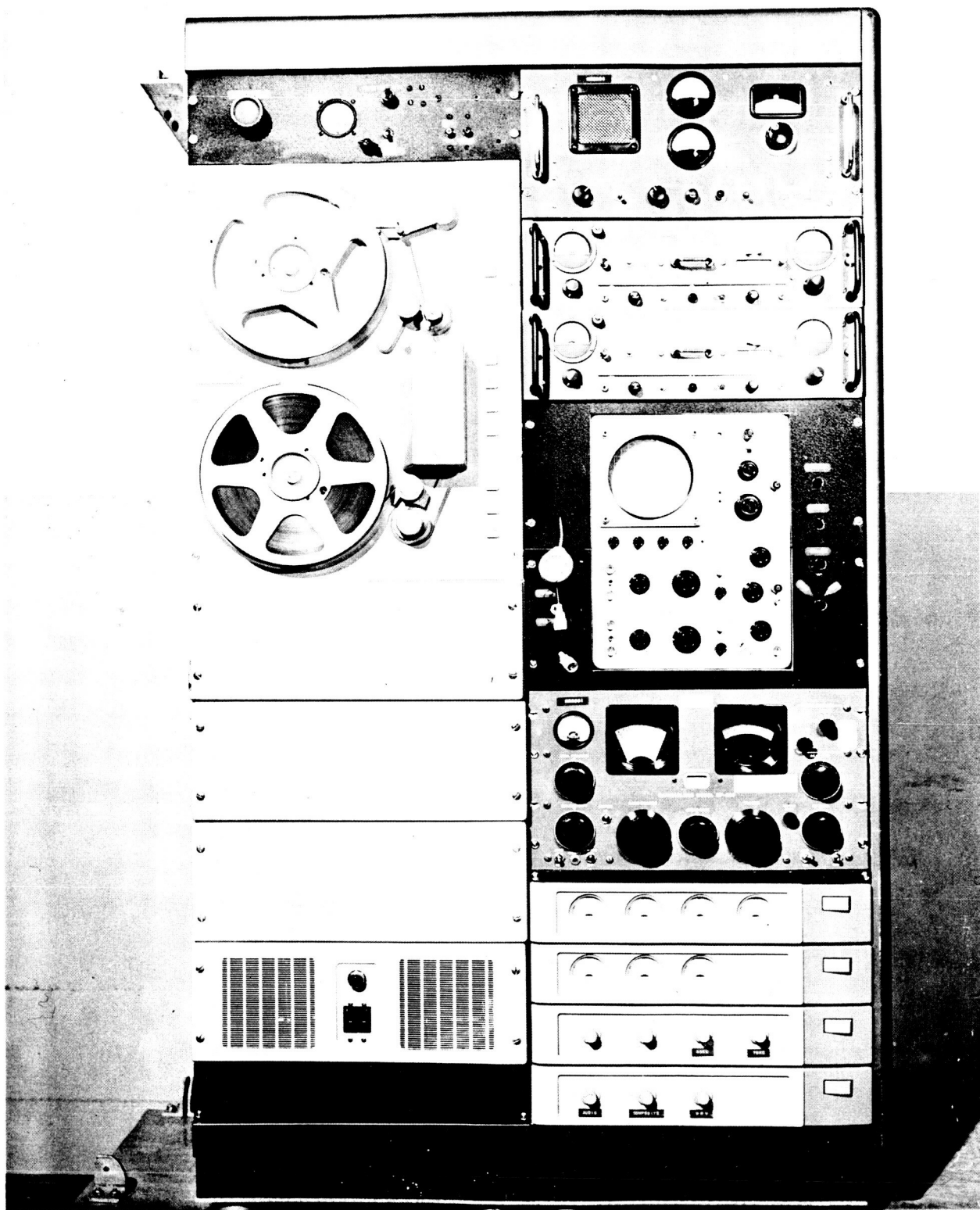


Figure 42. The Airborne Receiving Station

TABLE V
AIRBORNE RECEIVING STATION EQUIPMENT

| <u>Item</u> | <u>Manufacturer and Model</u> |
|-------------------------------------|---|
| Receiver, telemetry | Nems Clarke Model 1670G |
| Receiver, communications | Hammarlund Model SP-600 |
| Recorder, magnetic tape, 7 track | Ampex Type FR-1100 |
| Oscilloscope, dual beam | Tektronix Model 502 |
| Amplifier, audio | Knight Model KN-510 |
| Discriminator (2), 40 kc, 70 kc | ElectroMechanical Research Model 67D |
| Cabinet, two section | AMCO Engineering Co |

II. EQUIPMENT CHECKOUT

Prior to departure for the test site, the airborne and ground stations were assembled as completely as possible. Late delivery of a few pieces of equipment prevented full scale checkout of the ground station. The most significant item was the FR-600 tape recorder, which was flown to the test site a week after the van arrived. The complete air station and as much of the ground station as available were checked for correct cabling, calibrated and run through a performance test with simulated telemetry signals. A few minor discrepancies required correction.

Upon arrival at Bemidji airport, arrangements were made to power the van, the stations were reassembled and other necessary preparations completed. When the FR-600 tape recorder arrived, it was uncrated and installed in the van. The considerable size and weight of the machine necessitated its partial disassembly and reassembly inside the van. After all the missing equipment had been delivered, both stations were thoroughly performance checked. The radiation detection systems were also checked and found to operate satisfactorily with one exception. A small detector furnished by the University of Minnesota provided a negative output which would not deviate the subcarrier oscillators properly. The sponsor furnished correct circuitry prior to the first flight.

III. PREFLIGHT PROCEDURES

Upon notification that a Class 2 or greater solar flare had occurred with a subsequent increase in atmospheric radiation, preparations for a launch were started. The tape recorder amplifiers and the discriminators were given a final tune up. Accurately measured DC voltages of 5 and 2.5 volts were fed into each subcarrier oscillator in turn, transmitted through the air, received in the ground station and recorded on tape. After the various detection systems had been secured to the balloon load bar, they were powered by a DC power supply and activated by placing suitable radioactive sources in the vicinity. The resulting simulated data pulses were recorded on the tape for about 10 minutes to assure correct operation of the devices. Load and no load battery pack voltages and transmitter output power were recorded in the project notebook. If, by the time these equipment checks were complete, the radiation level in the atmosphere had increased significantly and weather conditions permitted, the balloon launching procedures were started. Approximately 30 minutes before estimated release time, the transmitter and all the radiation detectors were started on battery power. Recording in the ground station commenced immediately. Figure 43 shows the balloon payload on the load bar just prior to launching.

IV. FLIGHT DATA MONITORING

After balloon launch, the telemetered data were monitored on the many devices available in the ground receiving station for this purpose. Each track on the tape recorder had its own oscilloscope on which could be displayed at the flip of a switch, either the incoming signal or that reproduced from the tape. A larger oscilloscope was available for examining or photographing individual data tracks. Approximately hourly the information from each detection system plus a time signal was recorded on a Visicorder strip chart. The strength of the composite telemetry signal was recorded on a Texas Instruments rectilinear recorder. Figure 44 shows the abortive first flight in its entirety on the right and the final two hours of the third flight on the left. The signal is suitable for recording down to one microvolt on the scale.

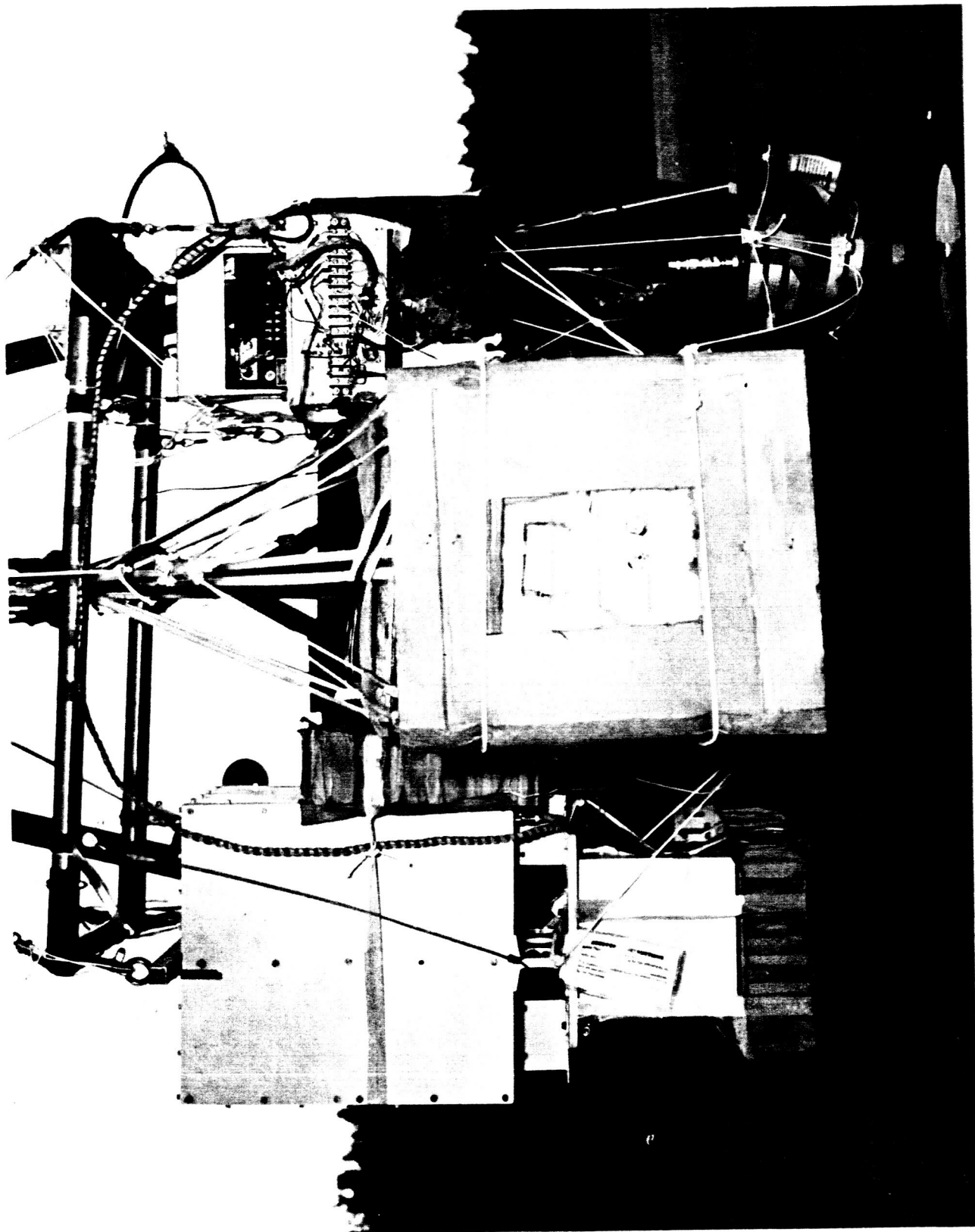


Figure 43. Balloon Payload Ready to Launch

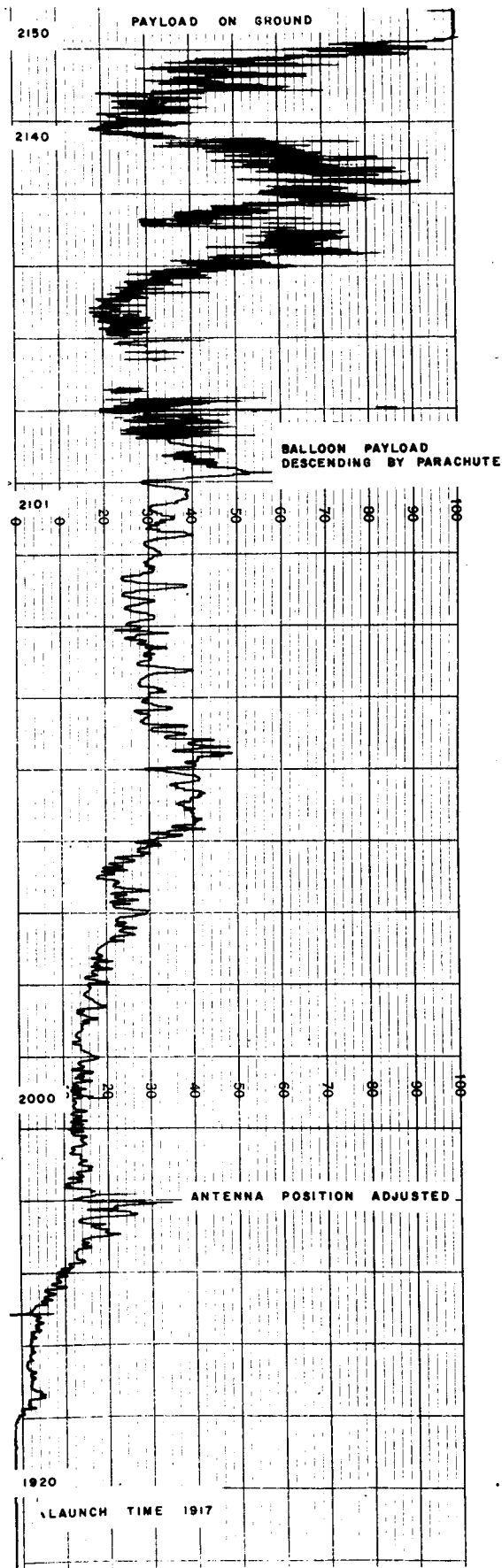
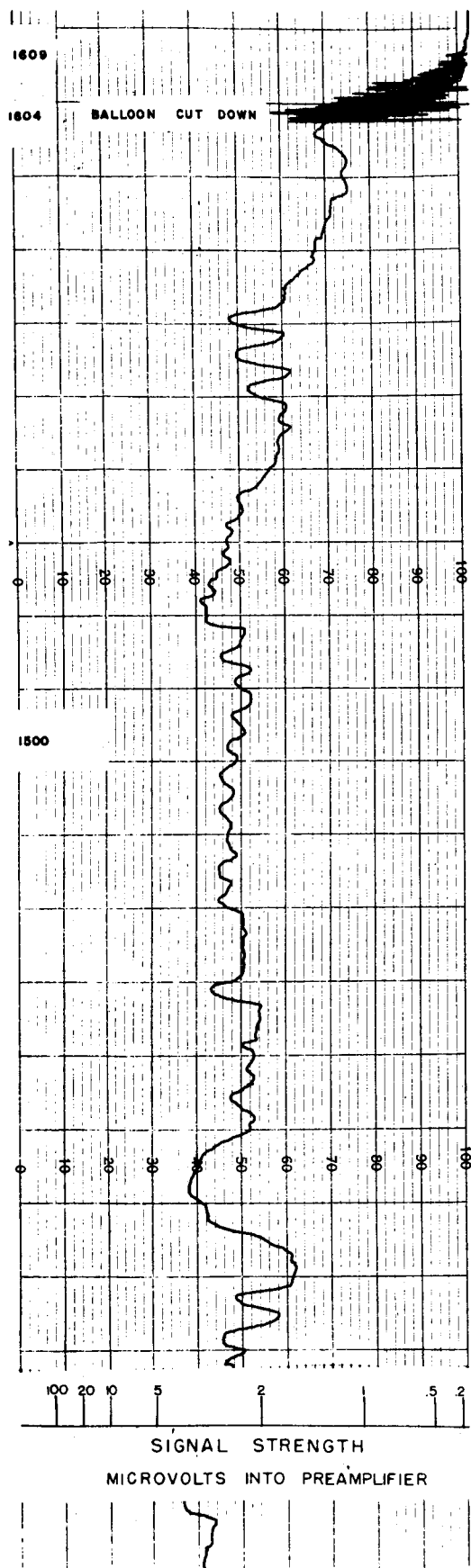


Figure 44. Signal Strength Recordings (Left: Flight 3, Right: Flight 1)

APPENDIX C

BALLOON CONSTRUCTION AND PAYLOAD WEIGHTS

I. BALLOON CONSTRUCTION

On Flight 1 the balloon was made from 3/4 mil polyethylene with 150-pound test reinforcing load tapes heat sealed along each of the 125 gores. The volume of this balloon was 13,446,154 cubic feet, based on a University of Minnesota balloon design formula, with a shape factor of 0.4. The gore length was 450 feet and the maximum diameter was 332 feet. The finished balloon weight was 1,332 pounds. This balloon was equipped with an inflation tube made from 2-mil polyethylene, 20 inches in circumference and 85 feet long. This tube was attached 24 feet from the top. Two appendices were provided for free lift exhaust. These were made from 20 feet circumference polyethylene, 123 feet long, entering the balloon 112.5 feet above the base and attached along the gore.

The balloon was made from top quality balloon grade film at Raven Industries under maximum quality control and inspection procedures. An analysis of samples of the material and individual seal samples was performed. No evidence of unsatisfactory material or sealing technique was discovered. It has not been possible to establish either the cause or mechanism for failure of the balloon.

On flight 2 the balloon used was made from 3/4 mil polyethylene with 100-pound test reinforcing load tapes heat sealed along each of the 95 gores. The volume of this balloon was 6 million cubic feet based on University of Minnesota balloon design formula, with a shape factor of 0.4. The gore length was 344 feet and the maximum diameter was 253 feet. The finished balloon weight was 684 pounds. The balloon was equipped with an inflation tube of 2-mil polyethylene, 20 inches in circumference, and 73 feet long, attached 20 feet from the top. A single appendix was provided for free lift exhaust. It was 6 feet in diameter, 37 feet long, attached 86 feet above the base of the balloon, but not attached along the gore. This balloon was made by Raven Industries in April 1960.

The balloon used for Flight 3 was identical with that flown on Flight 2. It weighed 685 pounds and was also built in April 1960 by Raven Industries.

II. PAYLOAD WEIGHTS

The following lists provide weight of all elements carried as part of the flight train.

FLIGHT 1

| | <u>Pounds</u> |
|--|---------------|
| Balloon, 13.4 million cubic feet | 1,332.0 |
| Parachute, 38 feet | 23.5 |
| Termination timers and radio command receiver | 18.0 |
| University of Minnesota payload unit | 7.0 |
| Dr. Yagoda (AFCRL) payload unit | 4.0 |
| Load bar | 13.5 |
| Drive up ballast | 70.0 |
| Flight ballast | 100.0 |
| Control package, including photobarograph, radio command receiver, beacon, antenna, ballast control (follow up, dribble and radio command ballast) | 40.0 |
| Gondola and lid | 24.0 |
| Lockheed payload unit | 67.5 |
| Telemetry | 78.5 |
| AFSWC payload unit | 20.0 |
| Hughes payload unit | 4.0 |
| <hr/> | |
| Gross load | 1,802.0 |
| Free lift (13%) | 234.0 |
| <hr/> | |
| Gross Lift | 2,036.0 |

FLIGHT 2

| | <u>Pounds</u> |
|--|---------------|
| Balloon, 6 million cubic feet | 684.0 |
| Parachute 28 feet | 12.5 |
| Gondola and lid | 24.0 |
| Ballast (total) and controls | 180.0 |
| University of Minnesota payload unit | 7.0 |
| Dr. Yagoda (AFCRL) payload unit | 4.0 |
| Load bar | 13.5 |
| Control package, including photobarograph, radio command receiver, beacon, antenna and batteries | 40.0 |
| Lockheed payload unit | 67.5 |
| Telemetry | 78.5 |
| AFSWC payload unit | 20.0 |
| Hughes payload unit | 4.0 |
| | <hr/> |
| Gross load | 1,135.0 |
| Free lift | 148.0 |
| | <hr/> |
| Gross lift | 1,283.0 |

FLIGHT 3

| | |
|---|---------|
| Balloon, 6 million cubic feet | 685.0 |
| Parachute, 28 feet | 14.0 |
| Load bar | 13.0 |
| Hughes payload unit | 4.0 |
| Lockheed payload unit | 67.5 |
| Telemetry | 78.5 |
| SAM payload unit | 4.0 |
| Termination timers and radio command receivers | 14.5 |
| Beacon and antenna | 19.5 |
| Photobarograph | 12.0 |
| | <hr/> |
| Gross load | 912.0 |
| Free lift (14%) | 127.0 |
| | <hr/> |
| Gross lift | 1,039.0 |

DISTRIBUTION

| | | | |
|---|----|--|---|
| AFSC (SCGB-3) Andrews AFB Wash 25, DC | 2 | Central Intelligence Agency Wash 25, DC ATTN: OCR Mail Room | 2 |
| HQ USAF (AFRDR-LS) Wash 25, DC | 1 | USAFA (DLIB) USAF Academy, Colo | 2 |
| HQ USAF (AFCIN-M) Wash 25, DC | 1 | Institute of Aeronautical Sciences ATTN: Library Acquisition 2 East 64th St New York 25, NY | 1 |
| AFMTC (Tech Library MU-135) Patrick AFB, Fla | 1 | | |
| APGC (PGAPI) Eglin AFB, Fla | 1 | Commanding Officer Diamond Ordnance Fuze Laboratories ATTN: (ORDTL 012) Wash 25, DC | 1 |
| ESD (ESAT) L. G. Hanscom Field Bedford, Mass | 1 | Boeing Airplane Company Aero-Space Division Library 13-84 P. O. Box 3707 Seattle 24, Wash | 1 |
| AFFTC (FTOOT) Edwards AFB, Calif | 1 | | |
| AFSWC (SWOI) Kirtland AFB, NMex | 1 | Redstone Scientific Information Center U.S. Army Missile Command Redstone Arsenal, Ala | 5 |
| AFSWC (SWRB) Kirtland AFB, NMex | 1 | | |
| AU (AUL-6008) Maxwell AFB, Ala | 1 | Commanding General White Sands Missile Range New Mexico ATTN: ORDBS-OM-TL | 1 |
| ASTIA (TIPDR) Arlington Hall Station Arlington 12, Va | 10 | British Liaison Office Ordnance Mission White Sands Missile Range NMex | 1 |
| AEDC (AEOIM) Arnold AF Stn, Tenn | 1 | | |
| AMD Attn: Chief Scientist Brooks AFB, Texas | 1 | National Library of Medicine 8600 Wisconsin Ave Bethesda 14, Md | 3 |
| AMD (AMAP) Brooks AFB, Texas | 10 | Defense Research Member Canadian Joint Staff ATTN: Dr. M.G. Whillans Director of Biosciences Research Wash 8, DC | 1 |
| ASD (ASBMA) Wright-Patterson AFB, Ohio | 1 | | |

| | | | |
|--|---|---|---|
| Cornell Aeronautical Labs, Inc 4455 Genesee St Buffalo 25, NY | 1 | Commanding Officer U.S. Army Medical Research Lab ATTN: Psychology Division Fort Knox, Ky | 1 |
| USAF School of Aerospace Medicine ATTN: Aeromedical Library Brooks AFB, Tex | 1 | Commanding General Research and Development Div Dept of the Army Wash 25, DC | 2 |
| Defense Atomic Support Agency ATTN: DASARA-2 The Pentagon Wash, DC | 1 | Director Naval Research Laboratory Wash 25, DC | 1 |
| Director Armed Forces Institute of Pathology Walter Reed Army Medical Center ATTN: Deputy Director for the Air Force Wash 25, DC | 2 | Director Office of Naval Research Wash 25, DC | 2 |
| NASA ATTN: Biology and Life Support System Program 1520 H. Street NW Wash 25, DC | 1 | University of California Medical Center ATTN: Biomedical Library Los Angeles 24, Calif | 1 |
| NASA ATTN: Chief, Division of Research Information 1520 H Street NW Wash 25, DC | 6 | Director Walter Reed Army Institute of Research ATTN: Neuropsychiatry Division Wash 25, DC | 1 |
| Commander U.S. Naval Missile Center Point Mugu, Calif | 1 | Commanding General Engineer Research and Development Laboratories ATTN: Technical Documents Center Fort Belvoir, Va | 1 |
| Commander Naval Air Development Center ATTN: Director, AMAL Johnsville, Pa | 2 | Commanding Officer U.S. Naval School of Aviation Medicine Pensacola, Fla | 2 |
| Headquarters U.S. Army R&D Command Main Navy Building ATTN: NP and PP Research Br Wash 25, DC | 1 | The STL Technical Library Space Technology Laboratories, Inc One Space Park Redondo Beach, Calif ATTN: Document Procurement Group | 1 |
| | | Librarian National Institute of Health Bethesda, Md | 1 |

| | | | |
|--|---|--|---|
| Medical Records Section Room 325 Division of Medical Sciences National Academy of Sciences National Research Council 2101 Constitution Avenue NW Wash 25, DC | 1 | Princeton University The James Forrestal Research Center Library Princeton, NJ | 1 |
| Lockheed Missile and Space Biomedical System Development Division Sunnyvale, Calif | 1 | Government Publications Div University of New Mexico Library Albuquerque, NMex | 1 |
| Librarian U.S. Naval Research Center Bethesda, Md. | 1 | Life Sciences Group Northrop Corporation 1001 Broadway Hawthorne, Calif | 1 |
| Aviation Crash Injury Research A Div of Flt Safety Foundation 2871 Sky Harbor Blvd Sky Harbor Airport Phoenix 34, Ariz | 1 | School of Aviation Medicine USAF Aerospace Medical Center (ATC) ATTN: SAMDYNA, Capt Bruce H. Warren Brooks AFB, Tex | 1 |
| Director Langley Research Center NASA ATTN: Librarian Langley Field, Va | 3 | ASD (WWB) Wright-Patterson AFB Ohio | 1 |
| Librarian Quarterly Cumulative Index Medicus American Medical Association 535 North Dearborn St Chicago, Ill | 1 | Life Sciences Dept, Code 5700 U.S. Naval Missile Center Point Mugu, Calif | 1 |
| The Rockefeller Institute Medical Electronics Center 66th Street and New York New York 21, NY | 1 | ASD (ASBAT Library) Wright-Patterson AFB Ohio | 2 |
| NORAIR Division of Northrop Corp ATTN: Bioastronautics Branch 1001 East Broadway Hawthorne, Calif | 1 | Aerospace Medicine The Editor 394 So. Kenilworth Ave Elmhurst, Ill | 1 |
| New Mexico State University University Library University Park, NMex ATTN: Library | 1 | Chief, Pathology Dept Presbyterian - St Lukes Hospital ATTN: Dr. George M. Hass 1753 W. Congress St Chicago 12, Ill | 1 |
| | | Chief, Dept of Pediatrics University of Oregon Medical School ATTN: Dr. Donald Pickering 3171 S.W. Sam Jackson Park Road Portland 1, Ore | 1 |

| | | | |
|---|---|--|------------------------------|
| Chief, Pathology Dept Evanston Hospital ATTN: Dr. C. Bruce Taylor Evanston, Ill. | 1 | Institute of Laboratory Animal Resources National Academy of Sciences/ National Research Council 2101 Constitution Ave., N.W. Wash 25, DC | 1 |
| Director U.S. Naval Research Laboratory (Code 5360) Wash 25, DC | 1 | Dr. Deets Pickett 8505 Lee Blvd Leawood, Kans | 1 |
| The Decker Corp Advanced Life Sciences Div 45 Monument Road Bala-Cynwyd, Pa | 1 | Dr. Walter J. Frajola M-352 Starling-Loving Hall Ohio State University Columbus 10, Ohio | 1 |
| SSD (SSZB) AF Unit Post Office Los Angeles 45, Calif | 3 | Dr. John Rhodes Space Biology Laboratory University of California Medical Center Los Angeles 34, Calif | 1 |
| Life Sciences Dept Douglas Aircraft Co Missile and Space Systems Santa Monica, Calif | 1 | Dr. S. B. Sells Department of Psychology Texas Christian University Fort Worth, Tex | 1 |
| Literature Acquisition Dept Biological Abstracts 3815 Walnut St Philadelphia 4, Pa | 1 | | |
| | | <u>LOCAL</u> | |
| The Lovelace Foundation Dept of Aerospace Medicine and Bioastronautics 4800 Gibson Boulevard, S.E. Albuquerque, N Mex | 1 | MDNH NLO ARSA (Attn: Capt Gross) SRAT SRAS MDSA | 1 1 20 3 1 40 |
| School of Veterinary Medicine ATTN: Major D. Mosely Ohio State University Columbus, Ohio | 1 | | |
| Information Officer USAFE French Liaison Office APO 230 New York, NY | 1 | | |
| Dr. W. D. Thompson Department of Psychology Baylor University Waco, Tex | 1 | | |